AD NUMBER
ADC009970
CLASSIFICATION CHANGES
TO: unclassified
FROM: confidential
LIMITATION CHANGES
TO: Approved for public release, distribution unlimited
FROM: Distribution authorized to U.S. Gov't. agencies only; Foreign Government Information; MAR 1977. Other requests shall be referred to Director, Naval Research Laboratory, Washington, DC 20375.
AUTHORITY
ONR ltr, 31 Jan 2006; ONR ltr, 31 Jan 2006

AD-C009970

SECURITY REMARKING REQUIREMENTS

DOD 5200.1-R, DEC 78

REVIEW ON 08 MAR 07

CONFIDENTIAL

NRL Report 7996

Acoustic Propagation in the Labrador Sea
[Unclassified Title]

CARL R. ANDRIANI AND JOHN CYBULSKI

Large Aperture Systems Branch
Acoustics Division

March 8, 1977

NAVAL RESEARCH LABORATORY
Washington, D.C.

NATIONAL SECURITY INFORMATION

Unauthorized Disclosure Subject to Criminal Sanctions.

CONFIDENTIAL

SECURITY CLASSIFICATION OF THIS PAGE (When Data Entered)

REPORT DOCUMENTATION PAGE	READ INSTRUCTIONS BEFORE COMPLETING FORM
1 REPORT NUMBER (14) NRL [redacted]7996	2 GOVT ACCESSION NO.
3 RECIPIENT'S CATALOG NUMBER (9) Final rept.	
4 TITLE (and Subtitle) (6) ACOUSTIC PROPAGATION IN THE LABRADOR SEA (U)	5 TYPE OF REPORT & PERIOD COVERED A final report on one phase of a continuing NRL Problem.
	6 PERFORMING ORG. REPORT NUMBER
7 AUTHOR(s) (10) Carl R. Andriani and John Cybulski	8 CONTRACT OR GRANT NUMBER(s) (8)
9 PERFORMING ORGANIZATION NAME AND ADDRESS Naval Research Laboratory Washington, D.C. 20375 (11) 67pp.	10 PROGRAM ELEMENT, PROJECT, TASK AREA & WORK UNIT NUMBERS NRL Problem S01-38 Project R2408 (16)
11 CONTROLLING OFFICE NAME AND ADDRESS Department of the Navy Office of Naval Research Arlington, Virginia 22217	12 REPORT DATE March 8, 1977
	13 NUMBER OF PAGES 61
14 MONITORING AGENCY NAME & ADDRESS(if different from Controlling Office) Long Range Acoustic Propagation Propagation (LRAPP) Maury Center for Ocean Science Naval Research Laboratory Washington, D.C. 20375	15 SECURITY CLASS. (of this report) CONFIDENTIAL
	15a DECLASSIFICATION DOWNGRADING SCHEDULE XGDS-(1) & (3) -2006

16 DISTRIBUTION STATEMENT (of this Report)

Distribution limited to U.S. Government Agencies only; foreign information; March 1977. Other requests for this document must be referred to the Commanding Officer, Naval Research Laboratory, Washington, D.C. 20375.

17 DISTRIBUTION STATEMENT (of the abstract entered in Block 20, if different from Report)

18 SUPPLEMENTARY NOTES

19 KEY WORDS (Continue on reverse side if necessary and identify by block number)

Propagation
Transmission loss
Passive surveillance
Labrador Sea

20 ABSTRACT (Continue on reverse side if necessary and identify by block number)

(C) A LRAPP-sponsored transmission-loss survey of the Laborador Sea was made during July 1972 at the accustic frequency of 50 Hz. The objective was to provide data to guide any future extensive and detailed studies of the Labrador Sea which would be relevant to future surveillance systems. Transmission loss was obtained using Mk 61 and Mk 82 SUS charges (detonated at 18.3 and 91.4 m respectively) dropped from aircraft, with the signals received on ship-suspended hydrophones (305 and 914 m deep) and buoy-deployed hydrophones (1628, 2515, 3252, and 3706 m deep).

(Continued)

DD FORM 1 JAN 73 1473 EDITION OF 1 NOV 65 IS OBSOLETE S/N 0102-014-6601

251950

4/12

20. (Continued)

(C) A transmission-loss contour chart of the Labrador Sea is presented for the 914-m-deep hydrophone and 18.3-m-deep source. The relevance of the contours to passive surveillance is brought out in a hypothetical example that shows passive detection of a 150-dBμPa/Hz (dB re 1 μPa at 1 m in a 1-Hz band) source at 50 Hz with a detection probability of 0.5 or greater and a false-alarm probability of 10^{-6} is not obtainable (using typical signal processing) beyond the 85-dB contour (approximate range of 80 n.mi.). The reason for this "poor" performance is the high ambient-noise levels (87 dBμPa/Hz at 50 Hz). This is estimated to result from low transmission loss (not greater than 100 dB) over most of the area surveyed. This result leads to the important conclusion that determination of ambient-noise directionality is the most important factor in long-range passive surveillance in this area (the ambient-noise value in the example was assumed omnidirectional for lack of directional data). The effect of source and receiver depths are discussed; the optimum passive system depth is projected to be within the interval 200 to 900 m. Details of transmission loss vs range, sound-speed profiles, and bathymetric features are included, providing the required data to illustrate and support conclusions.

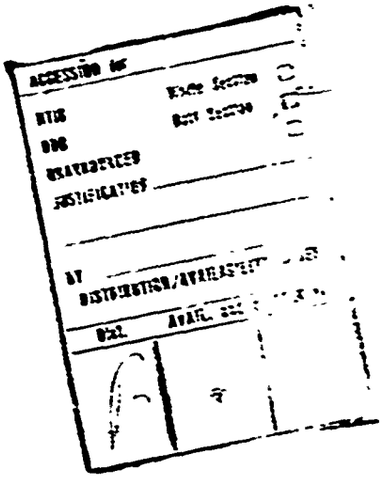

CONTENTS

ACKNOWLEDGMENTS

(U) This work was supported by LRAPP Program Office ONR Code 102-OSC, Dr. R. Gaui. Dr. B. Adams of NRL was the chief scientist during the phase of NORLANT 1972 covered by this work and collected these data. In addition Mr. Evan Wright (NRL) effected the computer programs and numerous other computations which provided all of the profiles shown in appendixes A and B. We acknowledge Messers D. F. Fenner and P. J. Bucca (NAVOCEANO) for use of the water-circulation portion of Fig. 3, Dr. Samuel W. Marshall (NRL) for Fig. 2, and Dr. W. B. Moseley (NRL) for Fig. A15.

ACOUSTIC PROPAGATION IN THE LABRADOR SEA
[Unclassified Title]

BACKGROUND

(U) The Long Range Acoustic Propagation Project (LRAPP), directed by the Office of Naval Research, has conducted a series of preliminary measurements and calculations to guide extensive ocean-area assessment which is to bear upon as many submarine-surveillance schemes as practical. These were multilaboratory (government and civilian) efforts directed at obtaining measurements on acoustic propagation, ambient sea noise, physical oceanographic parameters, submarine geology, and surface-ship surveillance. The data obtained, in addition to guiding further extensive measurements, provide the needed tests for the many physical models and computational techniques which predict the acoustic scenario that a specified system, in a specified environment, has to contend.

(U) The Navy has interest in pursuing this effort in that the measurements and calculations provide the basic, data-supported results necessary to the design and more importantly project performance of surveillance systems of present and future interest to the Navy's total ASW requirement and capability. An additional bonus is that these data provide a base against which to test a more basic research effort undertaken in other related programs.

(U) This particular LRAPP effort is related to ongoing efforts in system design and development within and of interest to the Navy. For example these data and calculations have direct bearing upon site selection, type of system in relation to the acoustic-environmental properties of the site, and expected performance for systems such as Fixed Distributed System (FDS), Surveillance Towed Array Sensor System (SURTASS), Moored Surveillance System (MSS), and Suspended Array Surveillance System (SASS).

(U) The NRL effort is in making measurements leading to estimates of transmission loss and ambient noise. Closely coupled are the model calculations made in the Labrador Sea, pursued so as to be directly related to the present and expected advanced development needs.

INTRODUCTION

(U) During July through September 1972 a comprehensive survey of the major acoustic and environmental characteristics related to passive surveillance of submarines in the Labrador Sea was made under the sponsorship of the Long Range Acoustic Propagation Project (LRAPP). This survey, known as *NORLANT 1972*, involved a multilaboratory effort to obtain data on acoustic propagation and ambient sea-noise for receivers located throughout the water column in midbasin, physical properties of the seawater

Manuscript submitted September 28, 1976.

affecting propagation, submarine geology, and the number and distribution of surface ships. The full scope of the survey and its objectives and a summary report of the partial results of this multilaboratory effort are given in Ref. 1.

(U) The objective of this work is to provide the surveillance community (and in particular, technical management) with data to guide any future extensive and detailed studies of the Labrador Sea which would be relevant to future passive surveillance systems such as Moored Surveillance System, Towed Array Surveillance System, and Suspended Array Surveillance System. These data are also useful for first-cut estimates of system performance and/or specification.

(U) As a participant in the NORLANT 1972 measurements, NRL concentrated its efforts on the measurement and modeling of transmission loss and ambient noise within the Labrador Sea. This report deals with the transmission-loss portion of the work. The ambient-noise results are the subject of a separate journal article [2].

EXPERIMENT OUTLINE

(C) NORLANT 1972 was a multiphase experiment, and only that portion relevant to transmission loss during Phase I (15 July to 29 July) will be discussed here. The complete details of the phase I experimental plans are given in Ref. 3. The ocean area of interest (Fig. 1) is bounded by North America to the west, Greenland to the north, the Reykjanes and Mid-Atlantic ridges from the northeast to the southeast, and the 40°N parallel. Included in this area are the approaches to the Davis and Denmark straits. The experiment involved four receiver locations designated A, B, C, and D as shown in Fig. 1 at about the 45°W meridian. Stations A, B, and C consisted of four hydrophones of an anchored ambient-noise-buoy (ANB) system (with hydrophones at depths of 1628, 2515, 3252, and 3706 m), and position D was occupied by the USNS *Hayes*, which suspended two hydrophones at depths of 305 and 914 m. The ANB receivers were high-gain units designed for the noise studies and for long-range transmission-loss data, and the *Hayes* receivers were low-gain units chosen primarily for transmission-loss work. The selection of buoy hydrophone depths is discussed in Ref. 2. Two U.S. Navy P3-C aircraft, modified to carry up to 384 "signals, underwater sound" (SUS) charges each, executed drop runs along the tracks shown in Fig. 1. Mark 61 SUS charges were dropped every minute, corresponding to an approximate range interval of 8.3 km, and detonated at a depth of 18.3 m. A Mark 82 SUS charge set to detonate at 91.4 m was dropped at 15-minute intervals, a range extent of 125 km. The explosive-sound level (integrated over the shot duration) was taken [4] as 204 dBre1μPa at 1 m in a 1-Hz band (dBμPa/Hz) at 50 Hz. The signals generated by the shots were recorded broadband aboard the *Hayes* and processed on line through 1/3-octave filters centered at 50 Hz with a Western Electric Company (WECO) shot processor [5]. The aircraft tracks were chosen to cover as much of those various regions of differing water mass and submarine topography which make up the Labrador Basin within the allotted time.

RESULTS

(U) The data taken on the 914-m-deep hydrophone on the *Hayes* for the 18.3-m-deep shots will occupy the major discussion. Data taken on buoy C and the *Hayes*

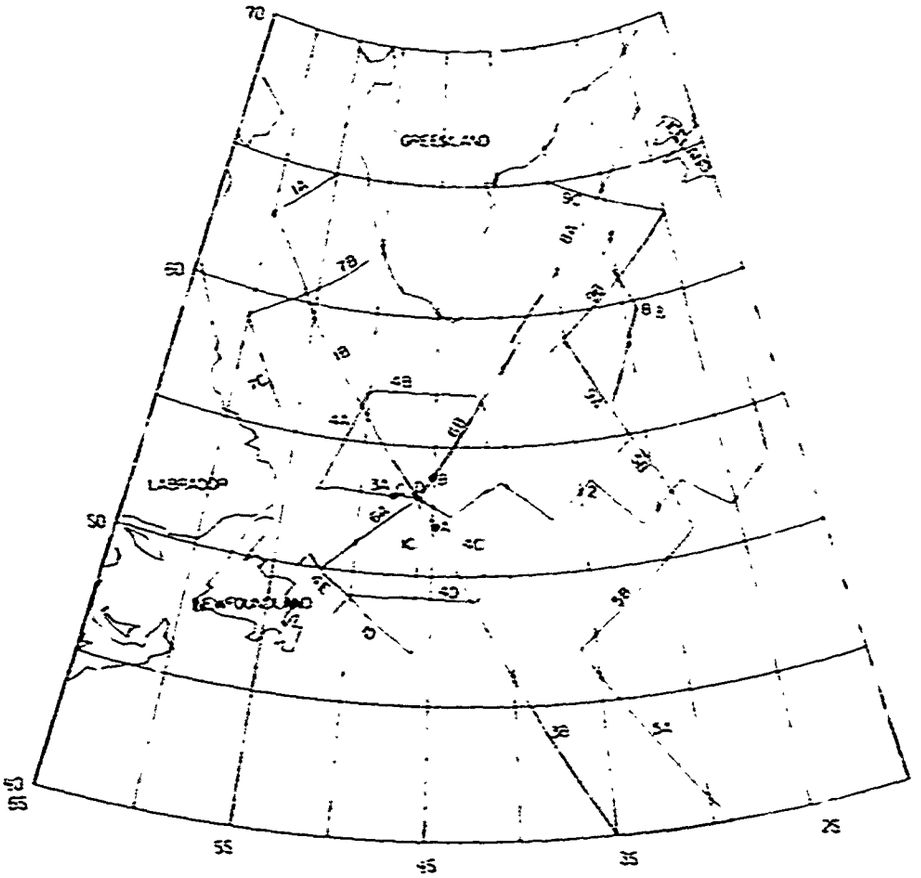

(C) Fig. 1 — Aircraft tracks

305-m-deep hydrophone will be brought in where appropriate. Since collection of these data was an objective of the survey, independent of the conclusions drawn herein, all of the acoustic and environmental data obtained are given in the appendixes.

Limits on Measurements

(C) The noise level on the 914-m *Hayes* hydrophone was limited by ambient sea noise for the entire experiment, and the 305-m receiver with a less compliant mount was low-level limited by surge and self-ship-generated noise. The average noise levels on the 914-m and 305-m phones at 50 Hz were measured at 87 and 102 dBμPa/Hz, respectively. Figure 2 shows the vertical distribution of the median of 791 10-minute averages (over 12 days) for ambient noise from the buoy at location C. The linear extrapolation to the surface (dashed line) appended to the figure will be used later. Based on these noise levels, the source level, and a required 3-dB signal-to-noise ratio, the maximum transmission loss is measurable to 114 dB and 99 dB on the 914-m and 305-m hydrophones respectively. Since the bulk of the loss values were less than 100 dB, the *Hayes* data set

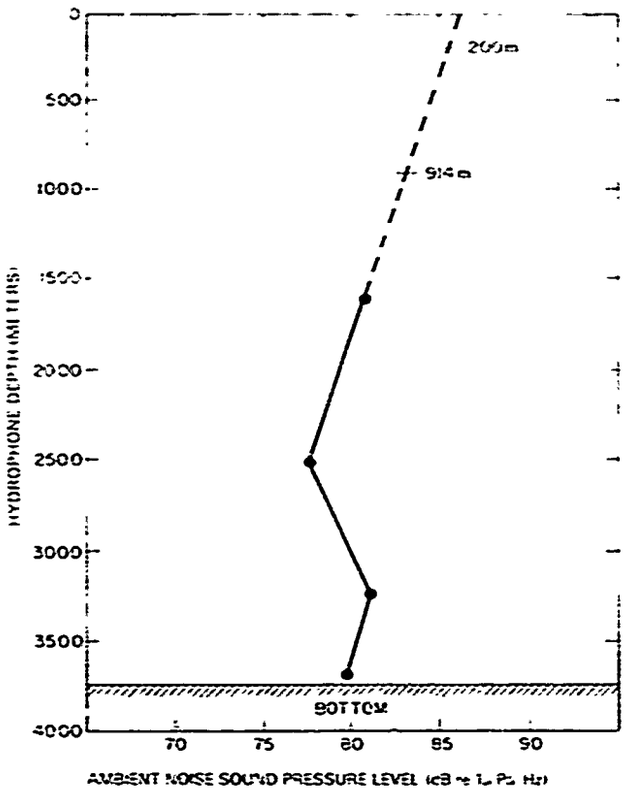

(C) Fig. 2 — Vertical distribution of ambient noise at buoy C (from Ref. 2)

was most extensively employed in the analysis. The maximum transmission loss to the buoy (117 to 122 dB) is determined by the noise level appropriate to the hydrophone depths, and the least loss is determined by the buoy overload point (approximately 15 dB above noise) and is 100 to 105 dB. From a sampling point of view, values outside these limits are possible and were observed. As a consequence the buoy data were used only for the long-range transmission-loss measures.

Transmission-Loss Contours

(C) Figure 3 is a composite chart showing the land masses, bathymetry, and major ocean currents in the experimental area. The aircraft tracks are also shown and can be identified readily with reference to Fig. 1. Of particular note are the Subarctic convergence (the heavy line), measured at 100 m in depth, and bathymetry encircling the Labrador Basin. The Subarctic convergence divides the basin into two distinct water masses and passes near the four receiving positions [6]. The velocity profiles to either side of this thermal front are clearly distinct (as evident from the second and fourth sound-speed profiles of Fig. A11, with the third profile being an example of the complicated sound-speed structure within the Subarctic convergence). It is the Subarctic convergence and

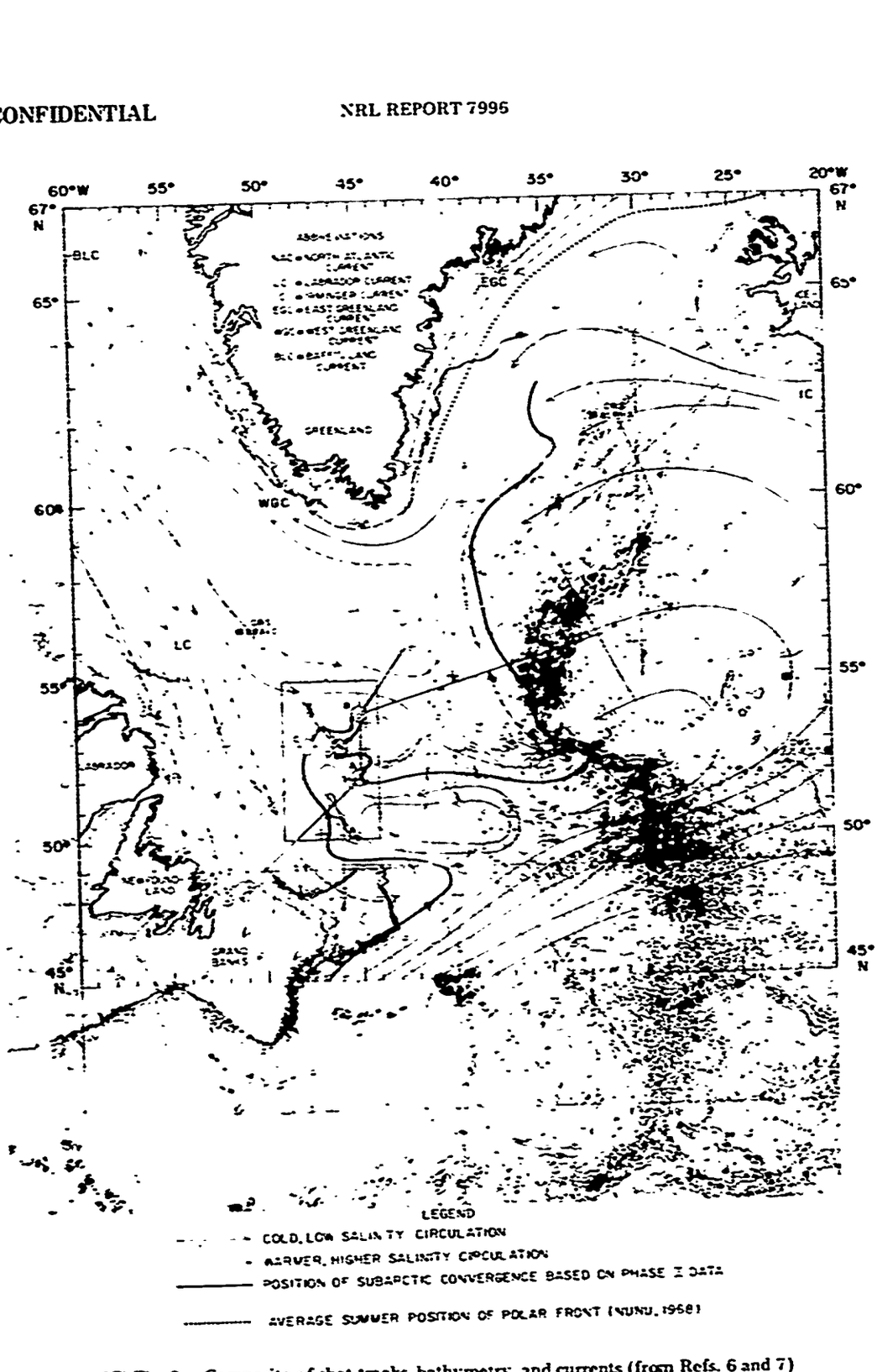

(C) Fig. 3 — Composite of shot tracks, bathymetry, and currents (from Refs. 6 and 7)

and those topographical features which rise above 2000 m which affect the transmission loss and its variability, as will be shown later. Two consistent effects seen throughout the data are a decrease of several dB in transmission loss along the continental slope ("slope enhancement," as explained in Appendix A in the section on track 3A and shown in Fig. A7) and a decrease in loss going from the warm to the cold side of the front and an increase going from cold to warm (section on track 3B and Figure A14 in Appendix A). The transmission-loss curves are relatively smooth and, as subsequent calculations show, predictable in the mean in most instances (section on track 1B and Figs. A1, A2a, and A2b in Appendix A).

(C) Analysis of the data taken on the shot runs shown in Fig. 1 have given rise to transmission-loss estimates along these lines. Based on the effects of topography, the water mass types, a regression analysis of transmission loss, and intensity calculations based on ray tracing [8], a transmission-loss contour plot was drawn for the 18.3-m source depth and is shown in Fig. 4. Location D is at the center of the contours for the *Hayes* 914-m-deep hydrophone. The solid line out from the land masses and outlining the Reykjanes ridge and Flemish cap represents the 1829-m depth contour. The dashed line at the lower right, indicates locations on the western side of the Mid-Atlantic ridge where the depth is about 1829 m. This region is characterized by a highly variable terrain.

(C) The solid contour lines indicate the data-base runs through or near these contours. These contours were generated using the data base, intensity calculations (ray tracing), and curve fits to the data (transmission loss versus range). The dashed contours indicate regions where the data base is sparse or inferential. These latter contours were generated by a combination of data extrapolation in range, intensity calculations based on ray tracing, and scientific deduction using the water sound-speed structure and bathymetry. As there was substantially good agreement between the calculated transmission loss as a function of range using ray tracing and the data base (sections in Appendix A on tracks 1B and 6A for example), the computations used to generate missing features of the contour plot have a high degree of confidence. Specifically, the intensity calculation was used due north of point D to fill in the gap between tracks 1B and 6B (Fig. 1), with a checkpoint where track 4B crosses. The following features of Fig. 4 are of particular note:

- The transmission loss is relatively low (100 dB) into the Davis and Denmark straits to ranges of 750 and 600 n.mi. respectively and to water depths shallower than 1829 meters.

- The loss abruptly increases from 100 to 105 dB to the southeast. Beyond this abrupt increase in loss to 105 dB, except for some acoustic windows, the propagation is blocked in many instances due to the effect of the warm North Atlantic current and topography which is shallower than the critical depth (there are many shallow areas in the foothills of the Mid-Atlantic ridge and significant size hills which block transmission, as described in the sections on tracks 3B, 5A and 5B in Appendix A).

- The Mid-Atlantic ridge also blocks transmission to the east, although it is apparent that acoustic windows exist (section on track 2 in Appendix A).

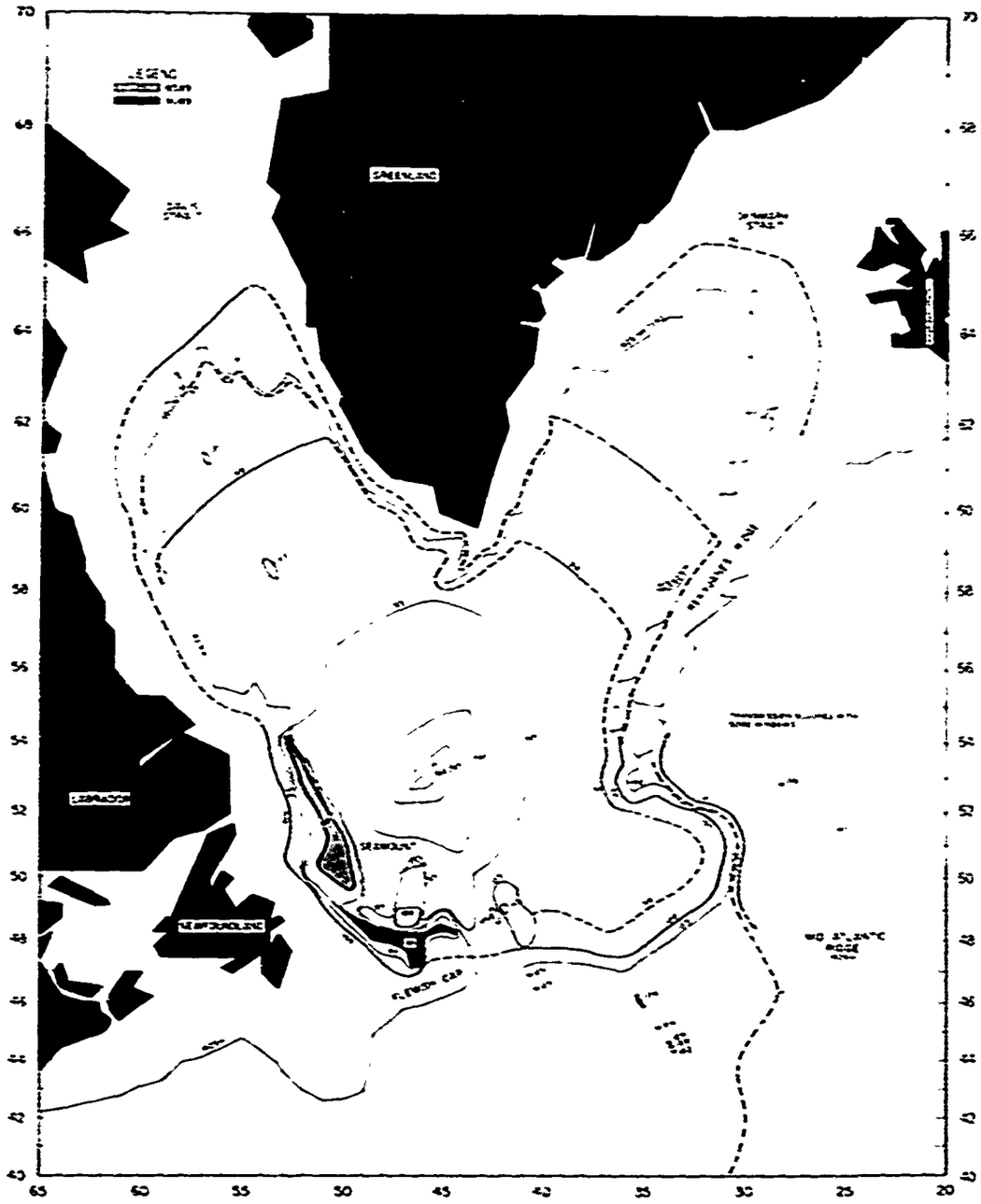

(C) Fig. 4 — Transmission-loss contours (dB) for an 18.3-m source (SUS) depth, 50 Hz, and 914-m hydrophone depth at 53° N, 46° W in the Labrador Sea for July

• The 85- and 90-dB contours which run along the continental slope and Flemish cap are due to slope enhancement. The magnitude of the enhancement is of the order of 5 dB (sections on tracks 3A and 6A in Appendix A).

• The variability in the contours to the south (in the vicinity of track 3B) is due to intersection of the track by the east-west-running Subarctic convergence (Fig. 3). The contour shows a high-loss area in the region crossing the front.

• The transmission loss falls off more rapidly with range in the direction of the Denmark strait than for the Davis strait. The reason is that the Subarctic convergence intersects the track toward the Denmark strait (track 6B), so that the sound-speed profiles show a broadening sound channel in this direction, whereas there is a strong channeling between source and receiver depths along the track up the Davis strait. This can be seen by comparing the sound-speed profiles in Fig. A1 (Davis strait) and A23 (Denmark strait).

• Due to the Mid-Atlantic ridge the transmission loss falls off to the east beyond the 95-dB contour, as evidenced by the bulges and closeness of the 98, 100, and 105 dB contours. The Charlie-*Gibbs* fracture zone which lies along this direction contains shallow regions (2000 m or less) and acoustic windows which influence transmission.

(C) Displacing the receiver to a more southerly and/or easterly direction would not particularly enhance transmission in these directions, as it is the topography and warm North Atlantic current water which results in high loss regions due to ray stripping by the bottom and path blockage. Thus data similar to these would have been obtained if the experimental site were taken further north and east of the actual site but still within the deep basin. If the site were moved near land masses of significant topographical features, differences in noise levels will almost certainly be found (as discussed in the Conclusions and Comments), affecting overall surveillance performance.

Transmission Loss to the 305-m-Deep Hydrophone

(C) To determine the difference in transmission loss to the 914-m and 305-m hydrophones for all tracks where data are available, a point-for-point transmission-loss difference was calculated. A one-sided test for the significance of the differences was made at the 95% and 99% confidence levels, since it is desired to test only if the 305-m loss values are greater than the 914-m loss values. The results are given in Table 1, where the entry "significant" in the last column means significance at the 0.05 level and the entry "probably significant" means significance at the 0.01 level. For example, for track 1A the deep hydrophone experiences a 3.5-dB greater loss than the shallow hydrophone, with a standard deviation of 1.2 dB. The table shows the difference between hydrophones not to exceed approximately 3 dB except for tracks 4D and 4E. These tracks are in part over the slopes, where enhancement occurs, and the difference reflects the differing levels of enhancement to each hydrophone. Also, track 4D is along the Subarctic convergence, and propagation to the shallower hydrophone is favored (Appendix A, section on track 2). The differences for tracks 4B, 4C, and 2 are not significant. Thus, if the contour lines of Fig. 4 are adjusted up by about 2 or 3 dB, the contours of this figure would represent the 305-m-deep hydrophone except in those regions of slope enhancement. However this change of 2 or 3 dB is not that significant in terms of an example of passive detection that is discussed later. Therefore construction of a contour chart for the 305-m-deep

(U) Table 1 — Comparisons of Transmission Loss to the Deep (D) and Shallow (S) Hydrophones

Track	Average Difference D - S, (dB)	σ (dB)	Number of Samples	Significance-Test Results
1A	3.5	1.2	19	Significant
1B	2.5	1.6	146	Significant
1C	1.4	1.9	78	Probably significant
1D	1.4	1.7	46	Probably significant
3A	2.5	1.7	56	Significant
3B	2.4	2.3	44	Significant
4A	1.2	1.6	58	Probably significant
4B	0.6	1.3	61	Not significant
4C	0.9	2.0	98	Not significant
4D	5.3	2.6	49	Significant
4E	6.2	4.1	26	Significant
2	1.5	3.7	57	Not significant
5A/5B	3.0	2.3	14	Significant

hydrophone would show differences relative to a chart for the 914-m-deep hydrophone that were neither significant nor give additional information to draw further conclusions. (The buoy data will be considered in the subsection Optimum System Depth.)

Transmission-Loss Dependence on Source Depth

(U) Shots set to detonate at depths of 18.3 m and 91.4 m were dropped simultaneously every 15 minutes along each track, or about 150 times for the entire exercise, for source identification, navigation checks, and dual-depth measurement. The shallow depth was favored, because it was expected to be more variable. To best show source/receiver depth differences in loss, the paired comparisons from all runs were combined and the difference data for a given receiver pooled into Table 2. These data are separated for the different depths of the shipboard and buoy hydrophones. A positive number in the middle colume indicates greater loss for the shallow shot.

(C) Table 2 shows that decrease in transmission loss of 3 to 5 dB may be expected in going from shallow (18.3 m) to deep (91.4 m) shots on the *Hayes* 305-m and 914-m hydrophones, dropping to 2.4 and 1.1 dB on the deeper buoy hydrophones. The reason for the improved transmission loss for the deeper shot is that it lies closer to the sound-channel axis. However the data for the individual tracks indicate this phenomena is directional in the basin, with some tracks indicating improved propagation as high as 7 dB and others as low as 1.5 dB. The size of the improvement depends on whether the depth

(C) Table 2 — Average Decrease in Transmission Loss For Deep Shots (d) Relative to Shallow Shots (s)

Receiver Depth (m)	s - d (dB)	No. of Samples
305	4.7	29
914	3.5	42
1628	2.4	11
2515	1.1	10
3252	1.5	14
3706	1.3	9

difference of 73 m moves the source significantly closer to the sound-channel axis. North of the Subarctic convergence, with a shallow axis, the effect is large, whereas southward, beyond the North Atlantic current, the deeper axis makes this difference with source depth less pronounced.

Optimum System Depth

(C) With regard to the dependence of transmission loss on receiver depth, analysis of the *Hayes* and buoy data show the least loss was obtained on the 305-m-deep hydrophone, with progressively greater loss at greater depths. However the optimum depth at 50 Hz based on analysis of the sound-speed profiles and acoustic modeling is projected to be in the vicinity of 200 m. The decrease in transmission loss, relative to that at the 914-m depth, is expected to be 2 to 3 dB. In determining the optimum sensor depth, the vertical distribution of ambient noise must be considered. The extrapolated ambient-noise level between 914 and 200 m increases by approximately 2 dB (Fig. 2). Thus the reduction in transmission loss may be partially, if not totally, offset by the increase in noise. Seeking a lower noise level by increasing depth is not fruitful since the buoy-hydrophone data indicate that the transmission loss increases significantly with depth (about 12 dB more at 3252 m than at 914 m) whereas changes in ambient noise (not monotonic with depth, Fig. 2) are small. Based on this investigation, a receiver depth between 200 and 900 m would be optimum.

SIGNAL-TO-NOISE RATIO AND SYSTEM DETECTION POTENTIAL

(C) In evaluating these data, especially the noise values, supporting evidence from other studies merits review; for example, the ambient noise level on the 914-m-deep hydrophone was measured at 87 dBμPa/Hz at 50 Hz on the *Hayes*. The extrapolated value to 914 m from Fig. 2 is 83 dBμPa/Hz. A Labrador Sea ambient-noise value of 86 dBμPa/Hz was reported in Ref. 9 for the open ocean under conditions of heavy shipping. An average value of 85 dBμPa/Hz with a spread between 80 and 95 dBμPa/Hz is reported in Ref. 9 for data taken by sonobuoy at depths of 30 and 90 m in the

Labrador Sea during the measurements reported in this report. Hence the noise value of 87 dBμPa/Hz employed here is consistent with many independent measurements.

(C) Using a measured ambient noise level (N) of 87 dBμPa/Hz, signal-to-noise-ratio (SNR) contours can be generated from the transmission loss (TL) by the transformation

$$SNR = SL - (TL + N),$$

where SL is the source level. Thus, if one assumes a hypothetical +142-dBμPa target source level (SL) at 50 Hz, the SNR becomes

$$SNR = 55 - TL.$$

For the 100-dB-transmission-loss contour

$$SNR = -45 \text{ dB}.$$

Thus a passive system intending to detect a 142-dBμPa target transiting the 100-dB-loss area would be required to overcome a deficit of 45 dB (depending on false-alarm and detection-probability constraints) in SNR to perform adequately. For the 80-dB contour 25 dB would be required. As an example of the significance of these numbers, a towed passive system with standard spectrum-analyzer processing and a 40-element array would theoretically accomplish the following:

Spatial processing (40 elements)	= 16 dB
Temporal processing (0.1-Hz bandwidth)	= 10 dB
Incoherent integration, 10 min (5 log 60)	= 9 dB
Degradation in system performance	= –3 dB
Total System Gain	32 dB

SNR at the processor output (100-dB contour) = –13 dB
SNR at the processor output (80-dB contour) = +7 dB.

(C) For a signal known except for phase in Gaussian noise a SNR of approximately + 7.1 dB at the processor output is needed for detection with a detection probability P(D) of 0.5 when the false-alarm probability is taken at 10^{-6}. For a P(D) = 0.9, a SNR of + 8.1 dB is needed [10]. Thus, to attain the 0.5 and 0.9 detection levels at the 100-dB contour, an additional system gain of 20.1 dB and 21.1 dB respectively beyond that of the preceding example would be required. These detection levels would be attainable within the 80-dB contour. Therefore any system operating in the Labrador Sea with ambitions to detect passively out to the 100-dB contour would require a system gain in excess of the combined temporal and spatial processing gain stated above and to detect passively out to the 80-dB contour would require a system gain at least as good. For the 305-m hydrophone depth an improvement of 2 or 3 dB would be obtained. However 2 or 3 dB does not significantly change the detection performance of the example system and may be completely offset by an increase in noise level. The basis for the conclusions given thus far is the tacit assumption that the ambient noise is omnidirectional. However there is evidence [2] that the noise field is directional, due to the asymmetry of shipping in the Labrador Sea. Hence conclusive estimates on detection probabilities in the Labrador Sea and system specifications will depend on ascertaining the azimuthal directivity of the noise field and uniformity within the basin.

CONCLUSIONS AND COMMENTS

(C) From the preceding the following summarizing conclusions relevant to surveillance and future environmental measurements in the Labrador Sea can be drawn:

- The transmission-loss contours taken together with ambient-noise levels show that significant long-range detection potential over most of the Labrador Sea (essentially beyond the 80-dB contour) would require system improvements over the example by the order of 10 dB for increased temporal processing and an improvement in spatial processing by 10 dB. The spatial gain could originate from a longer array or with array advantage against directional noise which would allow midbasin detection out to the 100-dB contour. These possibilities are presently foreseeable.

- The optimum depth for a passive system in terms of maximum signal-to-noise ratio at this site is estimated to be between 200 m and approximately 900 m.

- There is no significant directional preference for transmission within the basin, if the southernmost boundary is north of the 47°N parallel and the Reykjanes and Mid-Atlantic ridges are boundaries to the east. Movement of the receiver to the north or east would not significantly change the transmission-loss results obtained from the experimental site. Therefore these data well represent site-independent transmission loss in the midbasin of the Labrador Sea. Site selection for a surveillance system in regions other than midbasin may provide advantages not otherwise obtainable. For example, placement of the receiver north and east of the experimental site in the vicinity of 56°N and 43°W may provide a 95-dB transmission-loss barrier simultaneously across the approaches to both the Denmark and Davis straits. Alternately, if the receiver were placed near the southern tip of Rekyjanes ridge, a barrier across the Denmark strait alone would be affected; an additional advantage is the reduced ambient noise in this region reported in ref. 1. From this point of view placement will be important. Again, the directionality of noise is important in determining location.

- The transmission loss up or along narrow regions of the continental slope is decreased on the order of 5 dB, providing low-loss zones along continental slopes and slopes leading to seamounts. The breadth (range extent) of the enhancement depends on the angle of the source track to the slope (Appendix A, section on trace 4A).

- Detection in the vicinity of the foothills of the Reykjanes and Mid-Atlantic ridges is projected to be sporadic at best, based on data samples every 4.5 n.mi., with the transmission being effectively cut off by rising topography to depths of 2000 m. This is especially true near the southern portion of the Mid-Atlantic ridge.

- Given that transmission loss to the south (beyond the 100-dB contour) and to the east (beyond the Mid-Atlantic and Rekyjanes ridges) is poor, the major component of ambient noise experienced is probably local due to shipping in the Labrador Basin. If so, this suggests that the directionality and seasonal variation of ambient noise depends to a large extent on the habits of fishing vessels off Labrador and Newfoundland [2].

- The transmission loss from a source near the sound channel as compared to snorkel depths is less to a receiving system at a depth between 300 and 900 m by 3 to 5 dB (and greater); hence the detection range increases for a deeper target.

RECOMMENDATIONS

(C) • Location of a receiver system should be studied in terms of forming a potential barrier across the Davis and Denmark straits simultaneously with a single receiver system (this may be possible without effective loss of coverage to the south).

(C) • Directionality of ambient noise should be examined in detail, since it may be the most important factor in system design, detection capability, and choice of location.

(U) • Prior to design or installation of any system in the area a wintertime estimate of both transmission loss and ambient-noise directionality should be made. Seasonal fishing vessels may be less abundant, lowering the ambient-noise level. Also the noise directionality can be different in winter.

(U) • More data should be acquired in the direction of the Denmark strait, because the data obtained during this experiment were not adequate to verify the transmission loss to the 1829-m contour.

(C) • Since transmission loss depends on direction as well as source depth, with variations between 2 and 7 dB, more data should be collected in directions of high interest for several source depths. These data will aid the design and evaluation of specific systems against expected target operating depths.

(C) • The conclusions drawn in this report are supported by midbasin measurements but the characteristics may be different near the basin boundaries. Hence noise measurements should be undertaken near the boundaries (such as along the Rekyjanes ridge) to determine existence of noise quieting [1] to levels lower than midbasin values.

REFERENCES

1. B. B. Adams (NRL) and R. L. Martin (NUSC), editors, "NORLANT, 1972, Preliminary Report" (U). Vols. I and II. Naval Research Laboratory, 9 Feb. 1973 (Confidential).

2. S. W. Marshall, "Mid-Water Ambient Noise and Signal-to-Noise in the Labrador Sea" (U), *J. Underwater Acous.* Mar. (1977). (Confidential).

3. J. Cybulski, "Operation Plan NORLANT, 1972, Phase I" (U), Naval Research Laboratory, 15 June 1972 (Confidential).

4. R. D. Worley, Bell Telephone Laboratories, private communication in 1971.

5. "Wave Form Convertor Operational Manual G.F. 44665", Western Electric Co., Winston Salem, N.C.

6. D. F. Fenner and P. J. Bucca, "Sound Velocity Structure of the Labrador Sea, Irminger Sea, and Baffin Bay during the Norlant-72 Exercise" (U), NAVOCEANO Technical Note 6160-06-73, Naval Oceanographic Office, Aug. 1973, and NOO TR-245, Nov. 1974 (Confidential). (Figure 2 of this report was loaned to the authors for use as an overlay for Fig. 3.)

7. Naval Warfare Planning Chart Base (NWPCB), North Atlantic Region (NAR) 1, 4, 5, 6, and 7, 1 Oct. 1969 (Confidential). (A composite of these five NAR charts were used as an overlay in Fig. 2 of this report.)

8. B. G. Roberts, Jr., "Horizontal-Gradient Acoustical Ray-Trace Program TRIMAIN," NRL Report 7827, Nov. 1974 (Unclassified).

9. "Oceanography For Submarines In the Labrador Sea" (U), Prepared Under the Direction of the Department of Defense and Published by the U.S. Naval Oceanographic Office, Report SP 121, Mar. 1972 (Secret).

10. C. W. Helstrom, *Statistical Theory of Signal Detection*, 2nd edition, Pergamon Press, New York, 1968.

11. W. B. Moseley, "Long Range, Low Frequency Acoustic Transmission Loss to Shetland" (U), Admiralty Research Laboratory, Teddington, Middelsex, ARL/0/R9, Jan. 1974 (Secret-Discrete).

FOREWORD TO APPENDIXES

(U) An objective of the NORLANT 1972 operation was to gather data representative of the acoustic and environmental characteristics of the Labrador Sea. Therefore all of the transmission-loss estimates derived from received signals, XBT's, AXBT's, and derived sound-speed profiles are given here. Appendix A contains these acoustic data and sound-speed profiles. Some of them are discussed in detail and illustrate the effects and support the conclusions drawn in the preceding text. Appendix B contains the XBT and AXBT thermal-structure plots. Appendix C discusses operations of the VP-24 squadron relative to SUS-charge and AXBT deployment, the AXBT data reduction, and surface-ship contacts.

Appendix A [Confidential]
TRANSMISSION-LOSS AND SOUND-SPEED-PROFILE DATA

(U) With liberal references to Figs. 1 and 3 of the main text, each of the shot tracks will be discussed in a generally counterclockwise order starting with 1B. All of the data given are with reference to the 18.3-m-deep source, except as noted, and is in a 1/3-octave band centered at 50 Hz.

TRACK 1B

(U) Track 1B runs from point D northwest up the Davis strait and traverses that water mass on the cold side of the Subarctic convergence. Point D is shown astride the Subarctic convergence, but it is probably closer to the warmer side. This can be seen in Fig. A1, which shows the sound-speed profiles as one proceeds from point D up to the Davis strait. The profiles show a narrow near-surface channel formed north of the Subarctic convergence which becomes increasingly pronounced toward the shallower northern portion of the track, where the cold near-surface Labrador current produces an exaggerated protrusion on the profile. These changes in profile reduce the transmission loss and improve propagation to the shallow depths of continental slopes (<1829 m) as evidenced in the figure. The transmission loss to the shallower hydrophone is consistently less than to the 914-m receiver, the average being approximately 3 dB over the entire track (Table 1). The transmission loss to the 305-m receiver follows an approximately 71.6 + 8.6 log (R/1 n.mi.) falloff with range based on a fit of the data to y = A + B log (R/1 n.mi.). The range R is in nautical miles from point D and y is the transmission loss in dB. An interesting feature is the comparative small scatter of the data. This small variability is estimated to result from the 1/3-octave-band processing and the large bottom excess, which provides many ray orders at all ranges. The residual standard deviation (s) to the preceding expression is ±1.6 dB. These data show a relatively smooth transmission-loss decay with range which is predictable in the mean with ray-trace techniques. This can be seen in Fig. A2a, which is the computed [8] transmission loss to the 914-m-deep hydrophone from along track 1B. The middle solid line is a least-square fit to the predicted loss values and is of the form y = A + B log (R/1 n.mi.), where R is the range in nautical miles. The bounding solid lines are 90% confidence limits on y. The mean of the computed and the experimental data agree to within approximately 3 dB. Figure A2b is a plot of the computed transmission loss to the 305-m-deep hydrophone and agrees in the mean, within 3 dB, with the acoustic data also.

(C) The transmission loss obtained from the buoy-C data for track 1B is shown in Fig. A3. There is a clear increase of transmission loss with depth, as can be seen in comparing this figure with Fig. A1. This effect is also seen clearly in other tracks (such as tracks 7 and 1D). The requirements for recording ambient noise on the buoys caused the shots to overload the system at source ranges less than 300 to 400 n.mi. Hence data points do not occur in the figure until approximately 350 n.mi., and the higher loss, deeper hydrophones become unsaturated first as range increases. The absence of data on

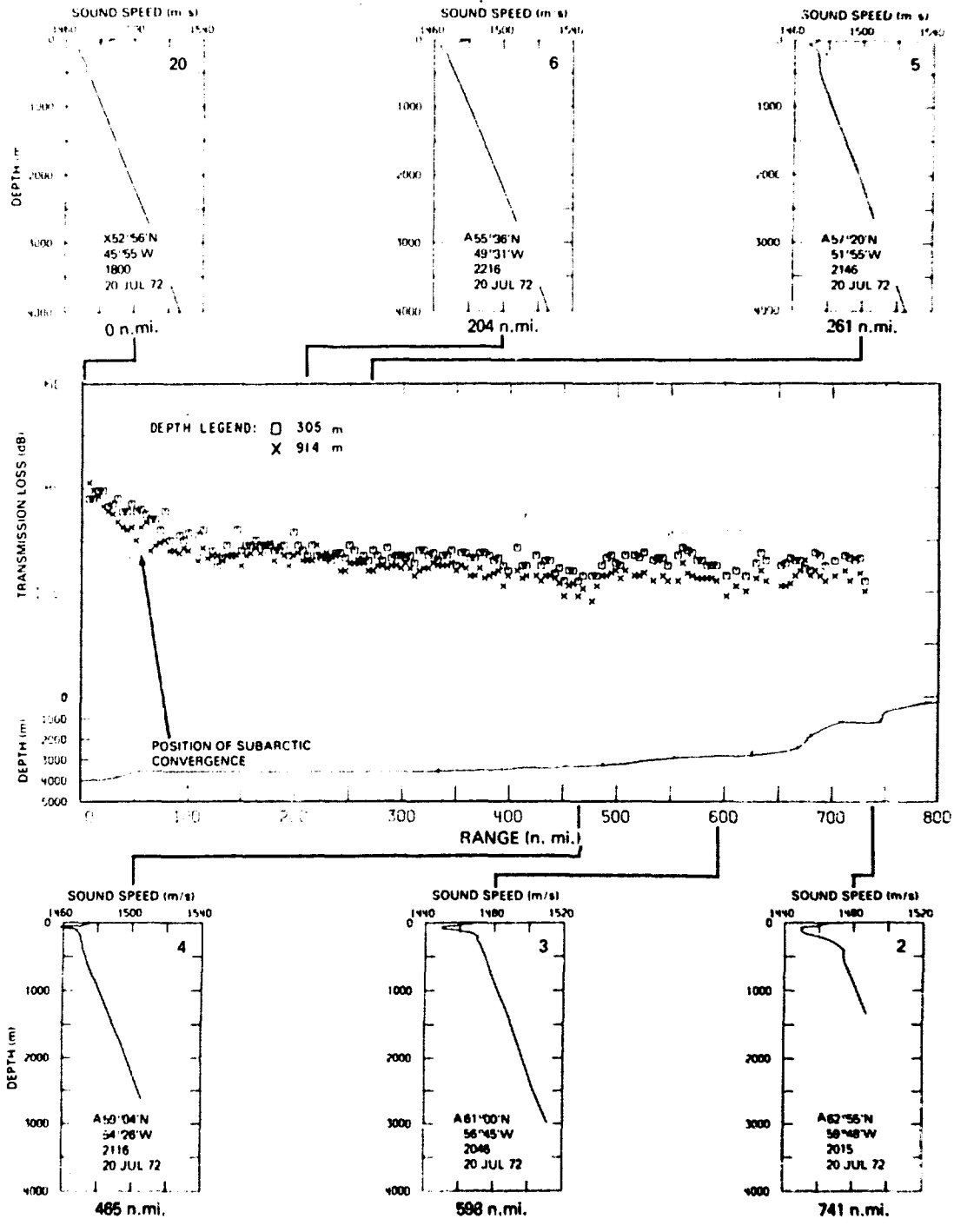

(C) Fig. A1 — Transmission loss from track 1B to the *Hayes* and sound-speed profiles. (The number in upper right corner of each sound-speed profile corresponds to the sequence of AXBT and XBT profiles in Figs. B2 and B3 respectively.

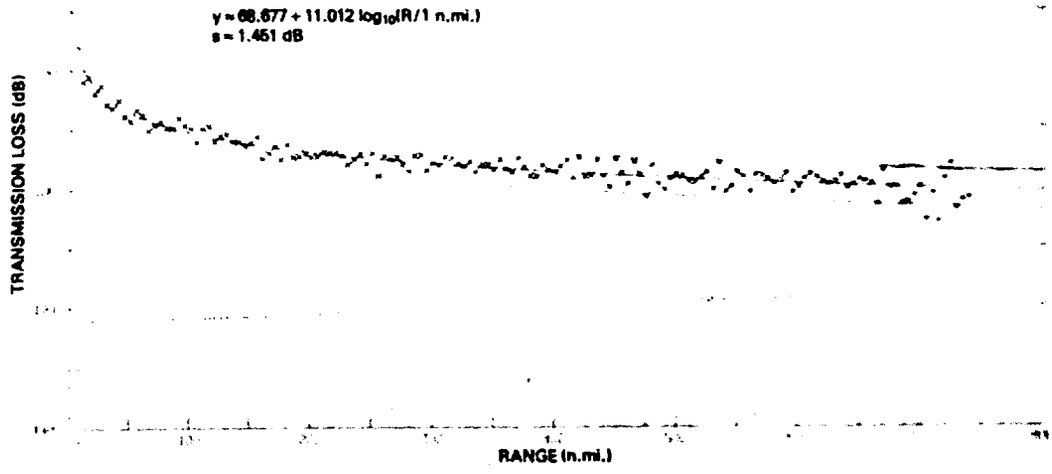

(U) Fig. A2a — Computed transmission loss from track 1B to the 914-m-deep hydrophone

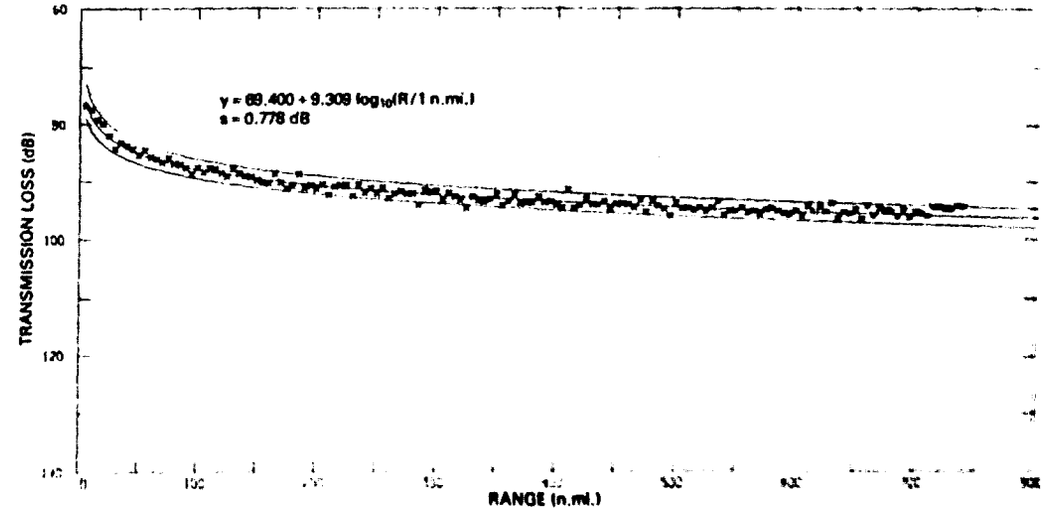

(U) Fig. A2b — Computed transmission loss from track 1B to the 305-m-deep hydrophone

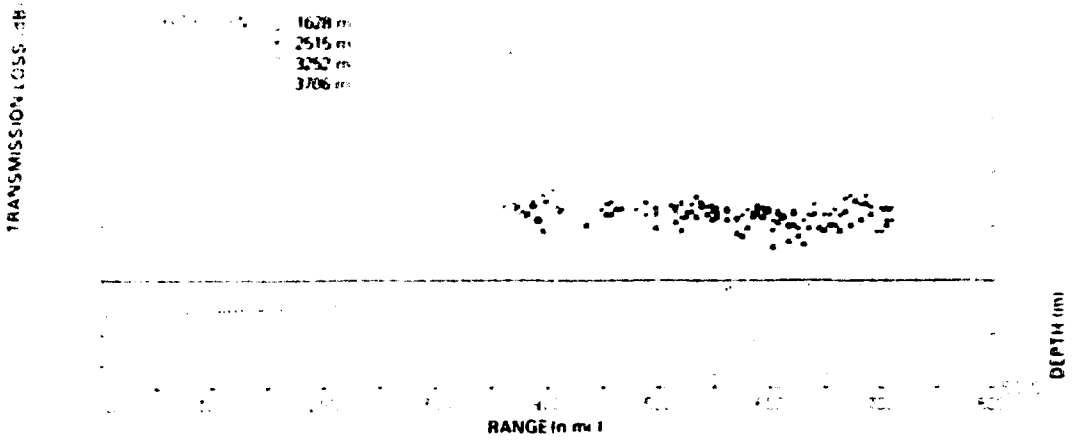

(U) Fig. A3 — Transmission loss from track 1B to the buoy

the deepest (3706 m) buoy hydrophone for most of the range was due to insufficient signal-to-noise ratio (SNR) for processing. As range decreases, the shallower hydrophones begin to overload and the SNR on the deeper hydrophones improves, so that processing is possible. Additionally, since only three processing channels were available, the three hydrophones with good SNR were processed. There is also some evidence of slope enhancement (explained in the section on track 3A) in the vicinity of 675 n.mi., at the 914-m-deep hydrophone and a buoy hydrophone. No such enhancement was observed on the 305-m-deep hydrophone, as bottom interaction was minor at the terminal range for the more shallow receiver.

TRACK 1A

(C) Transmission loss versus bearing for track 1A is shown in Fig. A4. This track is in water shallower than 1829 m in the Davis strait and illustrates the relatively low loss (<100 dB) to 750-770 n.mi. for both hydrophone depths. The several-dB difference in loss between the shallow and deep hydrophones is also seen. Transmission loss versus bearing to the buoy hydrophones is shown in Fig. A5, and again the loss is significantly greater to the deeper hydrophones than to the more shallow *Hayes* hydrophones. Also there is in general an increase in loss with depth on the buoy hydrophones themselves.

TRACK 7

(C) Track 7 data were taken on the buoy hydrophones only, and transmission loss versus bearing is plotted in Fig. A6. This plot shows a loss that is relatively flat with change in bearing and at a much lower level than would be expected on the *Hayes* hydrophones as evidenced in the portion of track 1B (Fig. A1) which intersects track 7 (at a range of 540 n.mi.). Again an increase in loss with hydrophone depth is apparent.

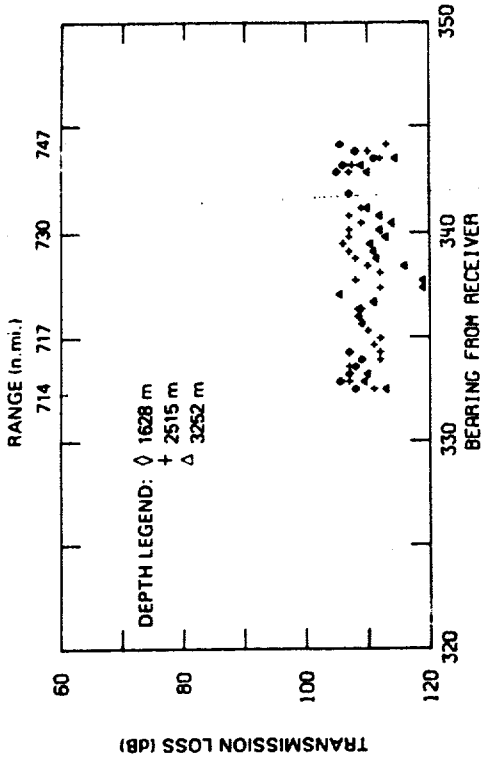

(U) Fig. A5 — Transmission loss from track 1A to the buoy

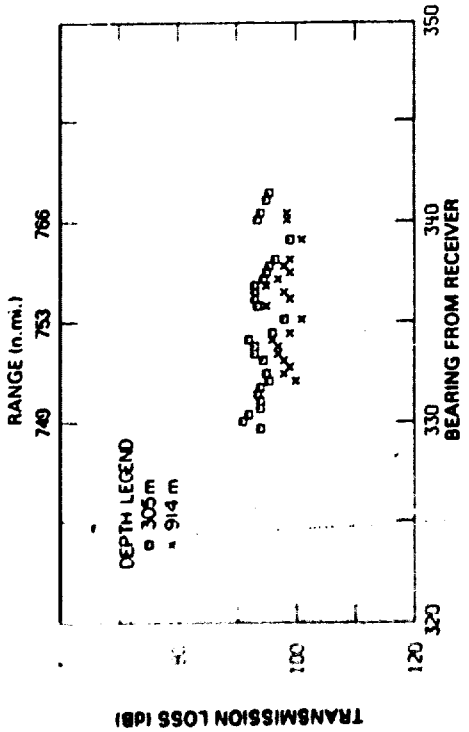

(U) Fig. A4 — Transmission loss from track 1A to the *Hayes*

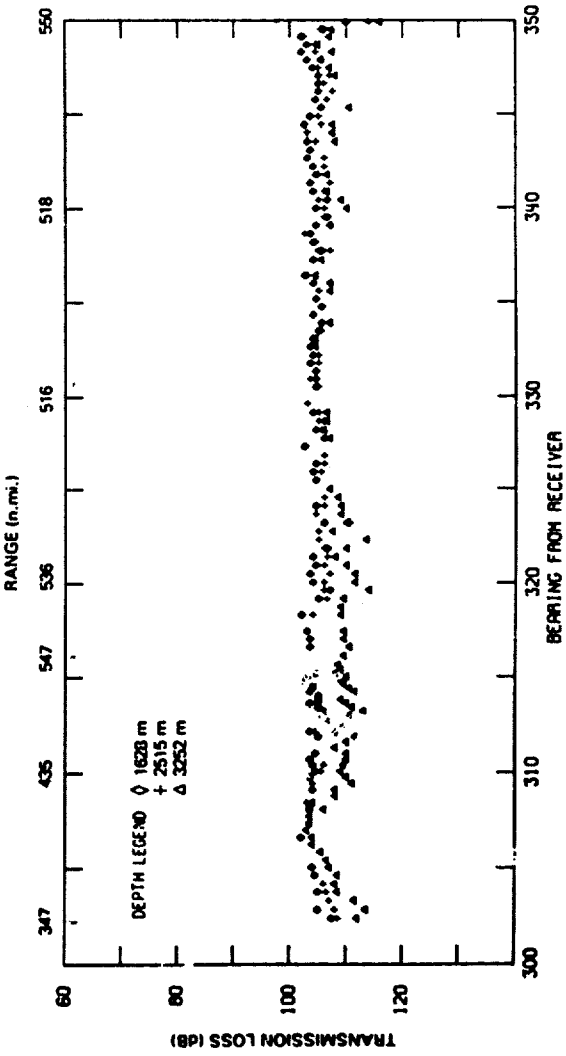

(U) Fig. A6 — Transmission loss from track 7 to the buoy

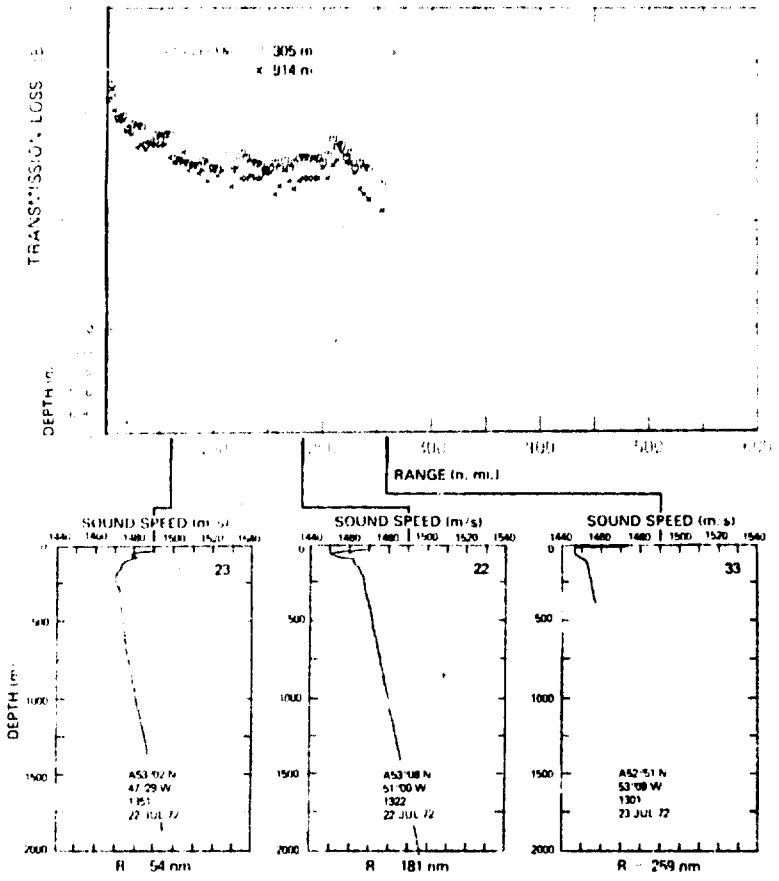

(C) Fig. A7 — Transmission loss from track 3A to the *Hayes* and sound-speed profiles

TRACK 3A

(C) The transmission loss from track 3A and sound-speed profiles are plotted in Fig. A7. The *Hayes* was on the warm side of and partially in the Subarctic convergence. The source transited the Subarctic convergence at approximately 50 n.mi. due west of the *Hayes*, where there is a flattening of the transmission-loss curve, and encountered a gradual continental rise at 75 n.mi., continuing until the bottom rises steeply to the shelf at 215 n.mi. The sound-speed profiles are similar to those along track 1B except for the considerable surface warming (third sound-speed profile) over the shelf. Hence the critical depth runs into the bottom, cutting off rays and producing sharp increase in transmission loss at the end of the plot. Of particular interest is the minima in transmission loss at about 220 n.mi. The minima is associated with the slope as the source progresses in the up slope direction. This effect is due to acoustic energy reflecting into refracted, surface-reflected (RSR) propagation (and is sometimes referred to as the megaphone effect).

(C) The enhancement for the 914-m-deep hydrophone occurs in the range interval 200 to 230 n.mi.; it is 5 dB at the extremum and is greater than 3 dB for a 12-n.mi. interval. The enhancement at the shallow hydrophone is about 4 dB for a total width of 25-n.mi. and is greater than 3 dB for approximately 6 n.mi. The ocean depth where the

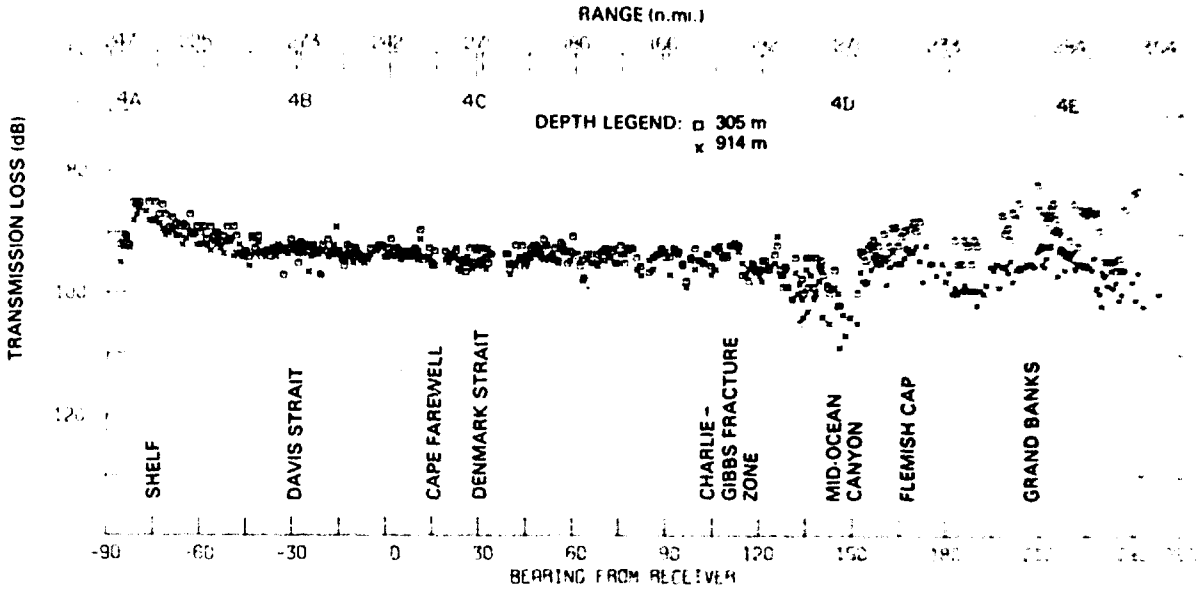

(U) Fig. A8 — Transmission loss from track 4 to the *Hayes*

enhancement occurs in 350 m. A feature of slope enhancement of interest in detection is that the detection probability will increase for a target transiting the slope, with the increase dependent on speed and angle relative to the slope. The dependence of enhancement duration on track angle will be discussed for track 4A.

TRACK 4A

(U) Track 4 is composed of five sections, as shown in Fig. 1 and marked 4A through 4E. The transmission loss is plotted as a function of bearing in Fig. A8, with ranges given at the top of the figure. Only the individual *Hayes* sections will be discussed, as the buoy was overloaded at the close ranges of track 4. In this section track 4A will be discussed.

(C) Track 4A intersects track 3A on the continental slope and experiences the same slope enhancement as in track 3A. Both the 914-m and 305-m receivers have minima 4 dB less than the loss to either side. The width of these minima are 46 and 50 n.mi. for the deep and shallow hydrophones respectively. The corresponding ranges for which the loss is 3 dB less are 11.5 and 12.3 n.mi. The loss at the termination of the enhancement (coming off the slope) is the same value, 93 dB, as for track 3A prior to running up the slope. Track 3A is more nearly perpendicular to the slope, whereas track 4A is at an angle, and this minimum range extent is thus broader. This result suggests that a submarine desiring to cross a slope can reduce its vulnerability to passive detection by crossing the slope normally to reduce time in the lower loss zone and, although counter to reducing this time, at a slower speed to reduce radiated noise. Also, if a submarine hovers over or cruises the slope area with the intention of avoiding detection by a shallow-water system, its vulnerability to a deep ocean system may increase. In this sense a deep-water system and a shallow-water system would compliment each other.

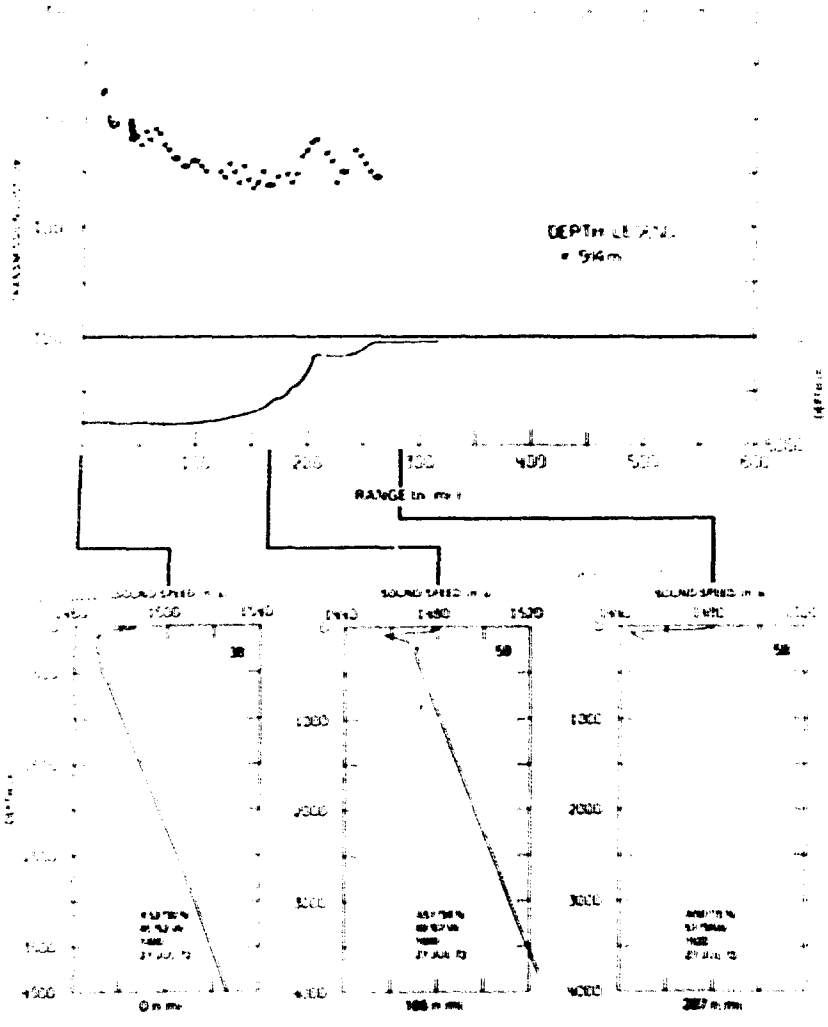

(C) Fig. A9 — Transmission loss from track 6A to the *Hayes* and sound-speed profiles

TRACK 6A

(C) Track 6A runs radially from point D toward Newfoundland. Data were taken on the 914-m-deep hydrophone only, after the *Hayes* had repositioned (as will be discussed in the section for track 6B). The track traverses the Subarctic covergence (Fig. 2) at approximately 90 n.mi. from point D. The transmission-loss curve and sound-speed profiles are shown in Fig. A9. The sound-speed profiles show the transition from the warm side to the cold side of the front. Two features of interest in this curve are the peaking in the curve at 200 n.mi. and again at 240 n.mi. These minima in transmission loss are associated with the double slope change as the track crosses the continental slope of Labrador. The first peak occurs in the range interval 188 to 228 n.mi. and is 6.5 dB above the trend of the previous portion of the curve; the peak remains 3 dB or more above this level for an extent of 24 n.mi. The second minima has a 5-dB reduction in loss and is 24 nm in extent, and it remains above 3 dB for 10 n.mi. The loss to all depths of the buoy receivers was less than 100 dB thus overloading the system over the entire extent of this track.

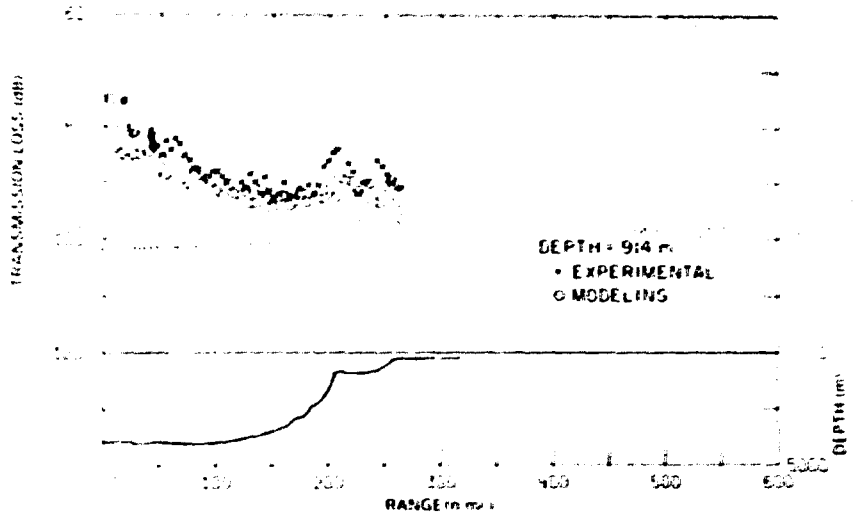

(U) Fig. A10 — Comparison of modeling with experimental transmission loss from track 6A

(U) Track 6A was selected to see how well slope enhancement can be represented by the intensity output from a ray-tracing model. During this effort it was evident that many rays would be needed to trace out the bottom encounters properly to obtain a sufficient number of paths for interpolations to the desired depths of interest. Therefore the type II output, an option of NRL's TRIMAIN computer code, was selected to get a distribution of intensity over the water column with fewer rays traced. It was conjectured that the bottom-loss class descriptors [A1] were not proper over the slopes for 50 Hz. Thus at about 180 n.mi. [A2] the loss class was reduced from 3 to 1; this brought out the peaks, as illustrated in Fig. A10. A reduction in loss class over the shorter range by at least one class level would provide even better agreement over this entire track. This is the direction recommended for frequencies below 100 Hz.

TRACK 1C

(C) The sound-speed profiles and transmission loss for track 1C are plotted in Fig. A11. The track crosses the Subarctic convergence near the Flemish cap, as evidenced by erratic sound speed in the third profile and the narrow surface channel in the fourth. The rise in bathymetry at 150 n.mi. may cause the depression in the transmission-loss curve between 180 and 250 n.mi., by blocking deep-going paths. Some slope enhancement is seen at both hydrophones between 310 and 330 n.mi. with a peak value of 4 dB. The minima remains withing 3 dB less loss than the surrounding region for 5 n.mi. Beyond the peak, the level on the deep hydrophone falls off rapidly, but the shallow hydrophone shows no significant increase in loss. The reason is that the shallow (narrow) surface channel near the Flemish cap connects the shallow source receiver by the near-surface paths, whereas the deep hydrophone at 914 m is below this duct.

(U) The buoy transmission-loss data over this range interval is shown in Fig. A12 and exhibits the greater loss seen on previous tracks, with slight evidence of slope enhancement by the deeper topography.

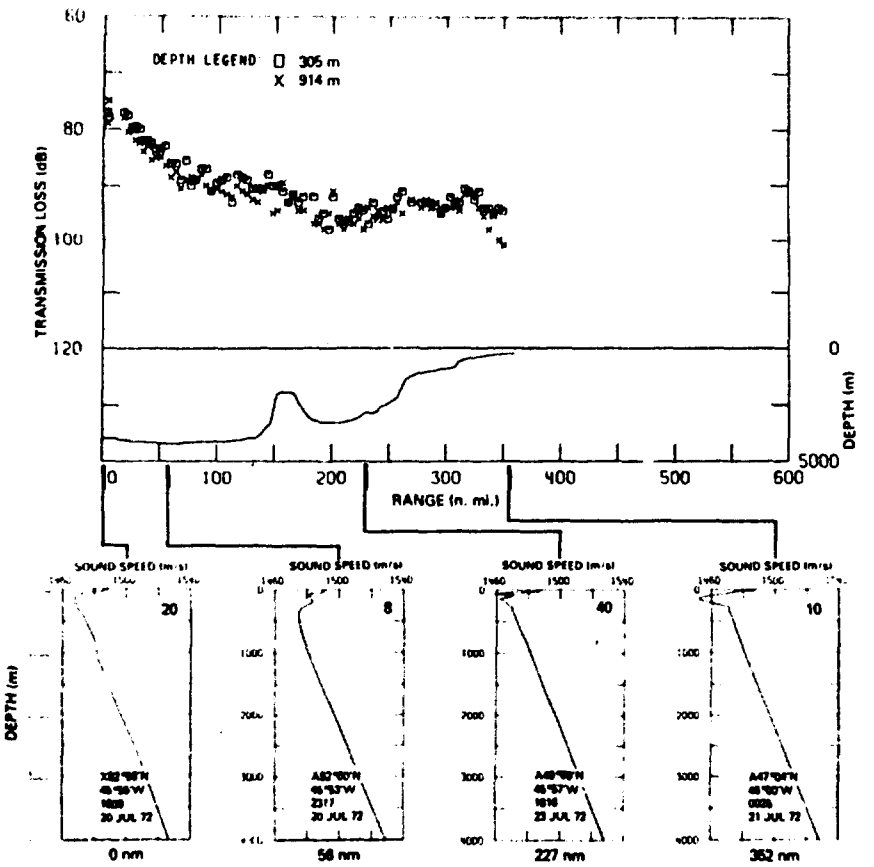

(C) Fig. A11 — Transmission loss from track 1C to the *Hayes* and sound-speed profiles

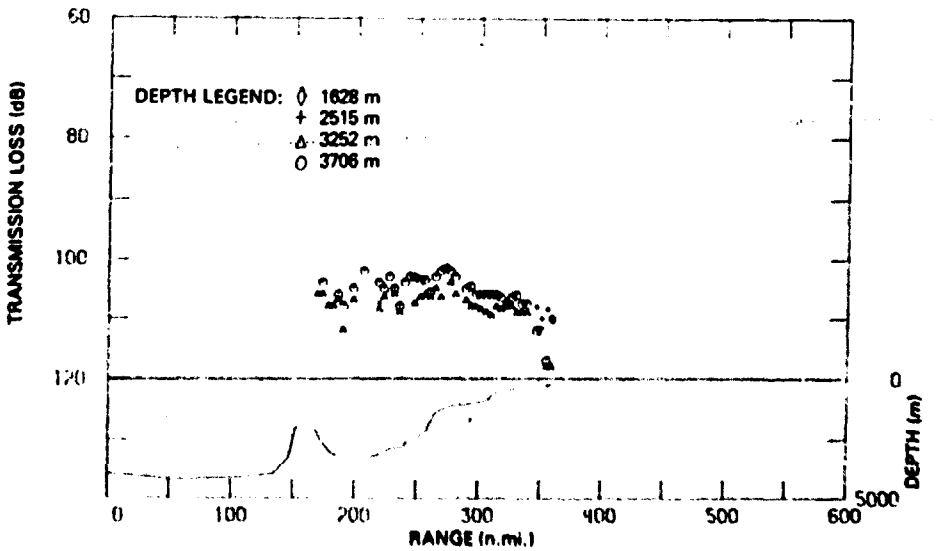

(U) Fig. A12 — Transmission loss from track 1C to the buoy

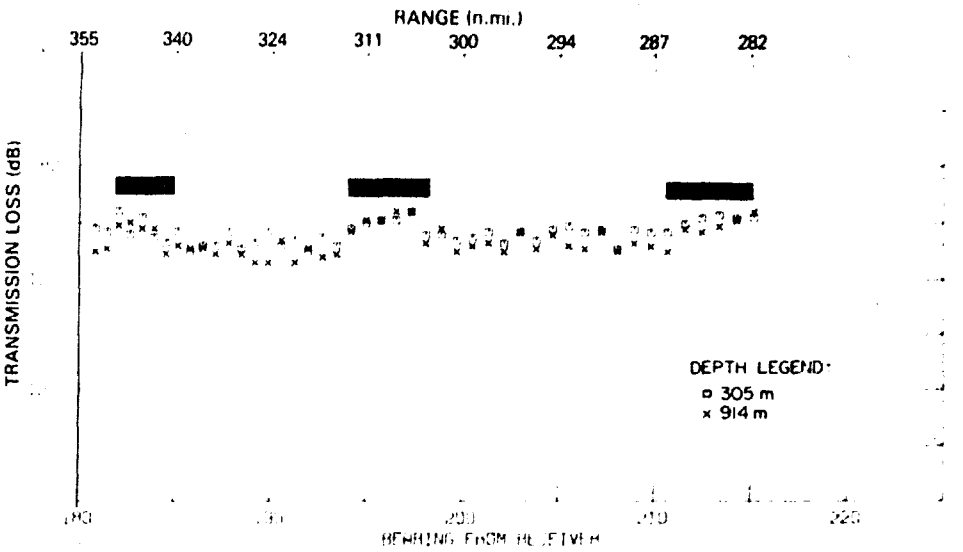

(U) Fig. A13 — Transmission loss from track 1D to the *Hayes*

TRACK 1D

(U) The transmission loss for track 1D is shown in Fig. A13 and is plotted as a function of bearing from point D, with the ranges of the source being given at the top of the graph. Large portions of track 1D are over the sloping terrain leading to the Flemish cap and continental rise; hence some of the track traversed regions suitable for slope enhancement. Three regions of enhancement are clear and occur on both hydrophones. Track 1D starts where track 1C ends, and the minima between 182° and 185° coincides with the slope leading to the Flemish cap, as seen in Fig. A11 near the end of track 1C. The second minima occurs between 194° and 198°, a range of 30 n.mi., which coincides with a high density of bottom-contour lines going from 400 to 800 m. The third occurs between 211° and 215° and is also associated with a sloping bottom.

(U) The transmission loss to the buoy is shown in Fig. A14. Here it is again seen that the transmission loss increases with buoy depth. The enhancements are displaced by about 10°, as governed by the relative positions of the buoy and the *Hayes*.

TRACKS 4D AND 4E

(C) Transmission loss for tracks 4D and 4E are plotted in Fig. A8 as a function of bearing, with ranges being given at the top. These tracks cover the bearing angles from approximately 150° to 245°. At 150° the track is parallel and just south of the Subarctic convergence, coinciding with the high loss at that bearing. Beyond 150° the slopes of the Flemish cap and the Grand Banks are crossed. There are two minima in the transmission-loss curve, with their characteristics being given in Table A1. Two points of interest about this curve are that the difference in transmission-loss between the shallow and deep hydrophones becomes large after approximately 212°, with the shallower phone exhibiting some 10 dB less loss on the minima, which are not coincident. As yet modeling effort has not addressed this particular data result to verify how the narrow surface

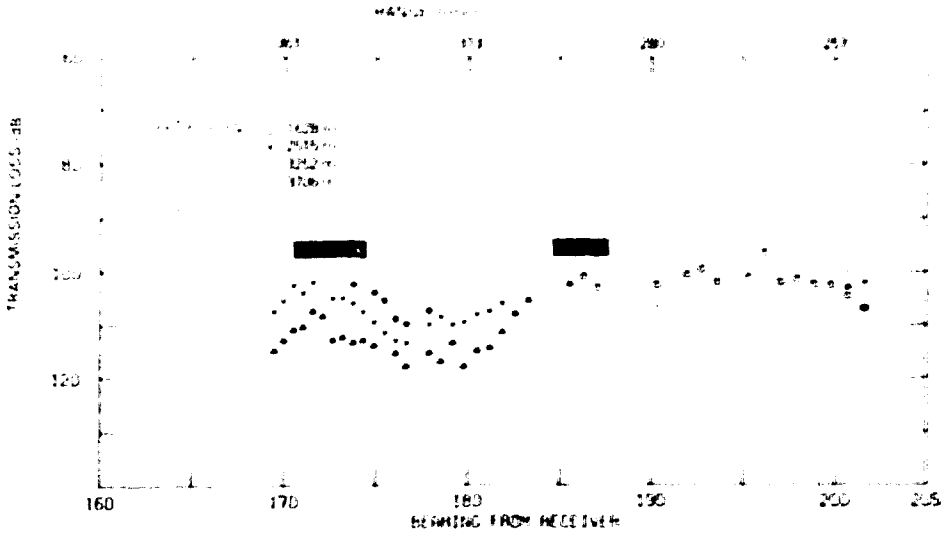

(U) Fig. A14 — Transmission loss from track 1D to the buoy

(U) Table A1 — Characteristics of the Transmission-Loss Minima in Fig. A8 for Tracks 4D and 4E

Hydrophone	Bearing (deg)		Decrease in Loss (dB)	
	First Minimum	Second Minimum	First Minimum	Second Minimum
Shallow	170	204	4.0	7.5
Deep	165	213	3.0	6.0

channel formed in the vicinity of the low-loss portion, as evidenced in the second sound-speed profile of Fig. A9, may account for additional low-loss paths between a shallow source and the receiver, at the same time that slope enhancement is occurring.

TRACK 3B

(C) Track 3B runs from point D to the southeast and terminates at the 40°N parallel. However data are shown only to a range of 475 n.mi. from point D (Fig. A15). Processing of the existing data beyond this range was not possible due to contamination by severe seismic interference off the Labrador Coast. This track cuts through the Subarctic convergence at two points as seen in Fig. 2 and marked by the vertical lines in Fig. A15. The transition from the warm through the cold and back to the warm side of the Subarctic convergence and the further warming that takes place to the south can be seen in the sound-speed profiles. The transmission-loss curve shown in Fig. A15 is complicated and appears to be composed of four segments. The first segment (0 to 150 n.mi.) falls off with a typical logarithmic dependence, flattening out between 100 and 150 n.mi. The second segment (150 to 260 n.mi.) falls off again with range but more steeply than

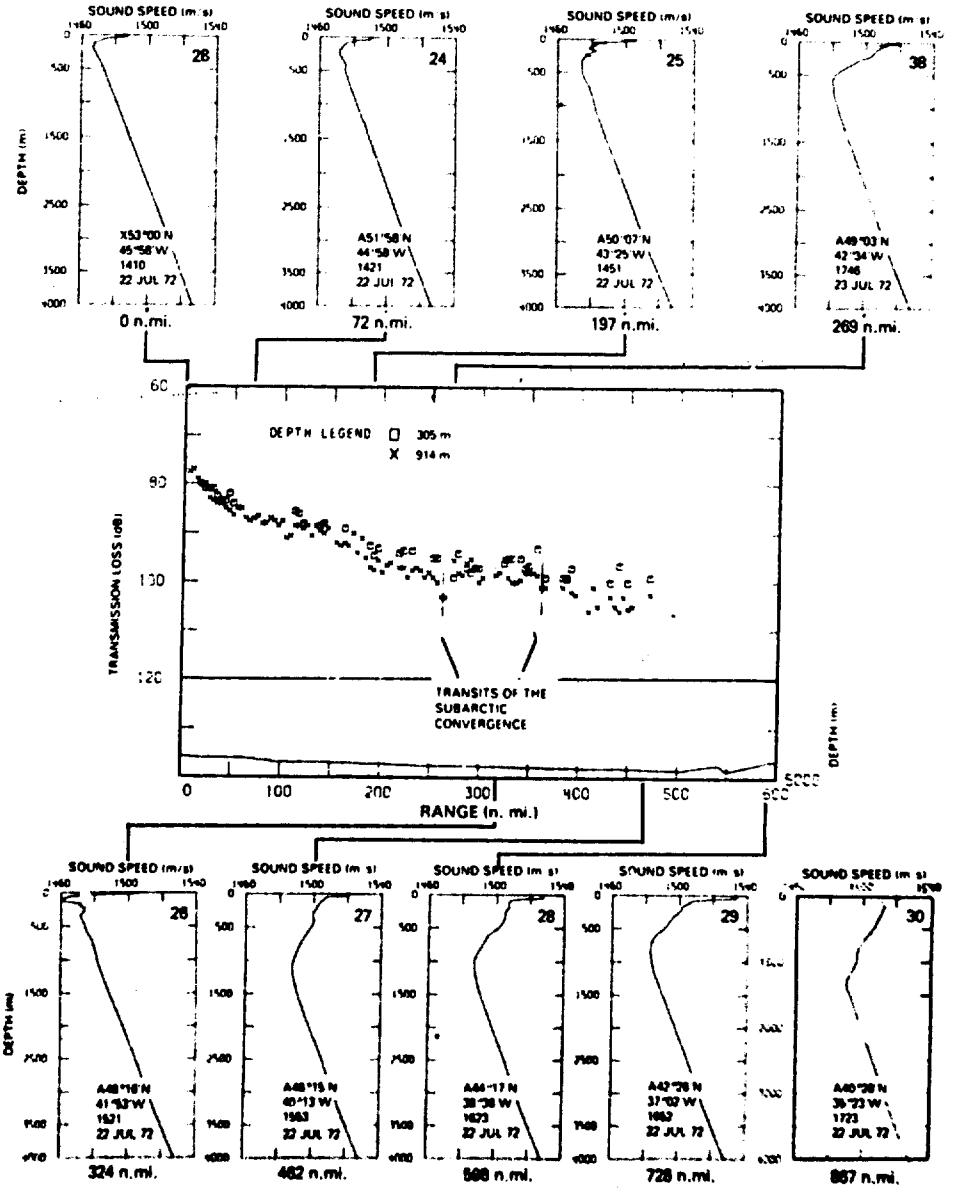

(C) Fig. A15 — Transmission loss from track 3B to the *Hayes* and sound-speed profiles

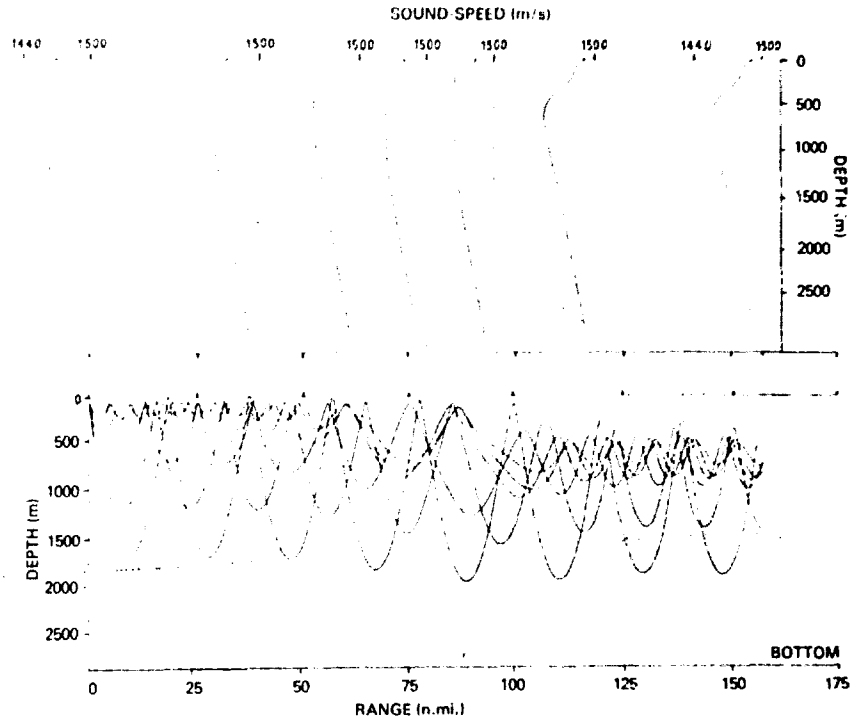

(U) Fig. A16 — Sound-speed profiles and ray diagram taken from Ref. A3

the first segment until 260 n.mi., where a sharp and narrow increase in loss occurs. The third segment (260 to 360 n.mi.) is an abrupt decrease in loss between transits across the Subarctic convergence (warm to cold at the first transit and cold to warm at the second transit). The decrease in transmission loss when transiting from the warm side to the cold side of the front is consistent throughout all the transmission-loss data; in particular there is an abrupt decrease in transmission loss at the transition from warm to cold at the beginning of track 4D (Fig. A8) and at 50 n.mi. on track 3A (Fig. A7). Segment 4 (360 n.mi. to the end) begins on the warm side of the Subarctic convergence and falls off almost in a continuation of the second segment. Although the track was 900 n.mi. long, data were obtained only to 475 n.mi. Some of these data were not received due to seismic interference. However, as can be seen from the last four sound-speed profiles, the water becomes markedly warmer and the sound channel increases in depth. Also, the critical depth intersects the bottom (not shown). The effect of this warming and the variable topography, which in many instances rises to depths of 2000 m, adversely affects and in many instances completely blocks transmission. The transmission loss in this direction falls off more steeply than for track 1B.

(C) The effect of transmission loss of sound propagating through a velocity field similar to that shown in Fig. A15 was investigated by Moseley [A3] and is illustrative of the phenomena experienced in track 3B. Figure A16 is taken from Ref. A3. Except for actual values of depth and sound speed the sound-speed profiles of Fig. A16 are similar to those of Fig. A15. The ray diagram, computed using the NRL ray-trace program TRIMAIN [8], show high-energy paths being channeled to deeper water as the source moves to the warmer profiles, explaining the poor coupling between the shallow source and receiver observed in track 3B at ranges greater than 500 n.mi. The additional complication with the Labrador Sea data is that the sound channel goes deeper for these data

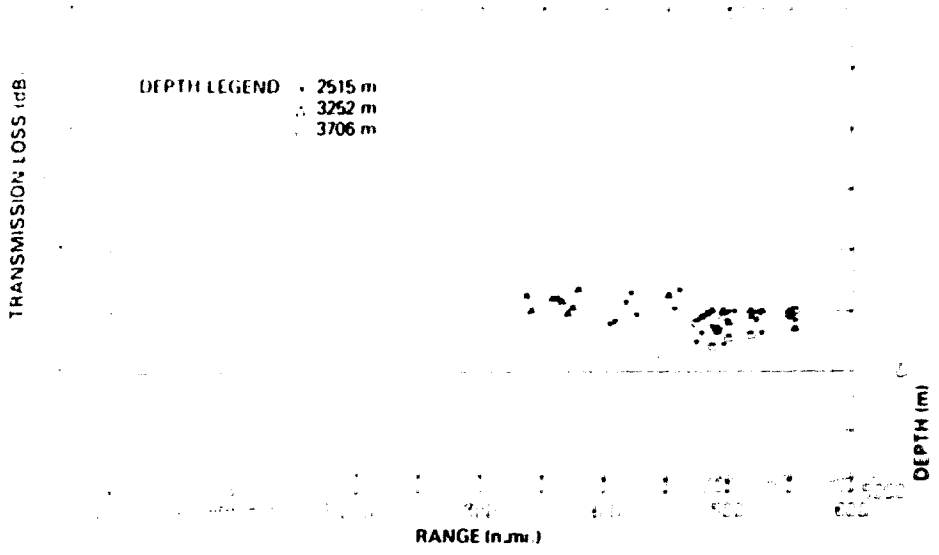

(U) Fig. A17 — Transmission loss from track 3B to the buoy

than in Ref. A3 and the rays interact with the bottom to some extent, further increasing the energy loss. Thus a deeper source would not necessarily exhibit significantly less loss, whereas near-surface ambient-noise sources would experience poor propagation into the Labrador Sea. The transmission loss to the deep buoy hydrophones shown in Fig. A17 was obtained out to 550 n.mi., a greater range than obtained by the *Hayes*, since the seismic interference in this instance was less pronounced on the buoy.

TRACK 5A

(C) The data are sparse along track 5A, as seen in Fig. A18. No data were processed beyond 700 n.mi. Review of the output of the analog monitor reveal some sporadic signals were received which were not processed due to seismic interference. However, based on the sound-speed profiles of Fig. A18, the discussion concerning track 3B, and the greater than 100-dB loss shown in Fig. A15, it is concluded that there are no paths with significant energy connecting the source and receiver. The transmission loss to the buoy is plotted in Fig. A19 with data having been obtained to 800 n.mi. before seismic interference precluded further processing. The data appear almost as a continuation of data for track 3B (Fig. A17).

TRACK 5B

(C) Transmission loss for track 5B is shown in Fig. A20. The gap in the data from the end of the track at 85° to 112° and from 112° to 122° is due in part to a high-level unidentified noise source in the vicinity of *Hayes* and to a lesser extent to blockage. Where data were obtained, the losses on the 914-m-deep hydrophone are in excess of 100 dB and on the 305-m-deep hydrophone are greater than 95 dB. The values greater than 100 dB are due to bathymetric interference and the warmer water encountered in this region, as discussed for track 3B and 5A.

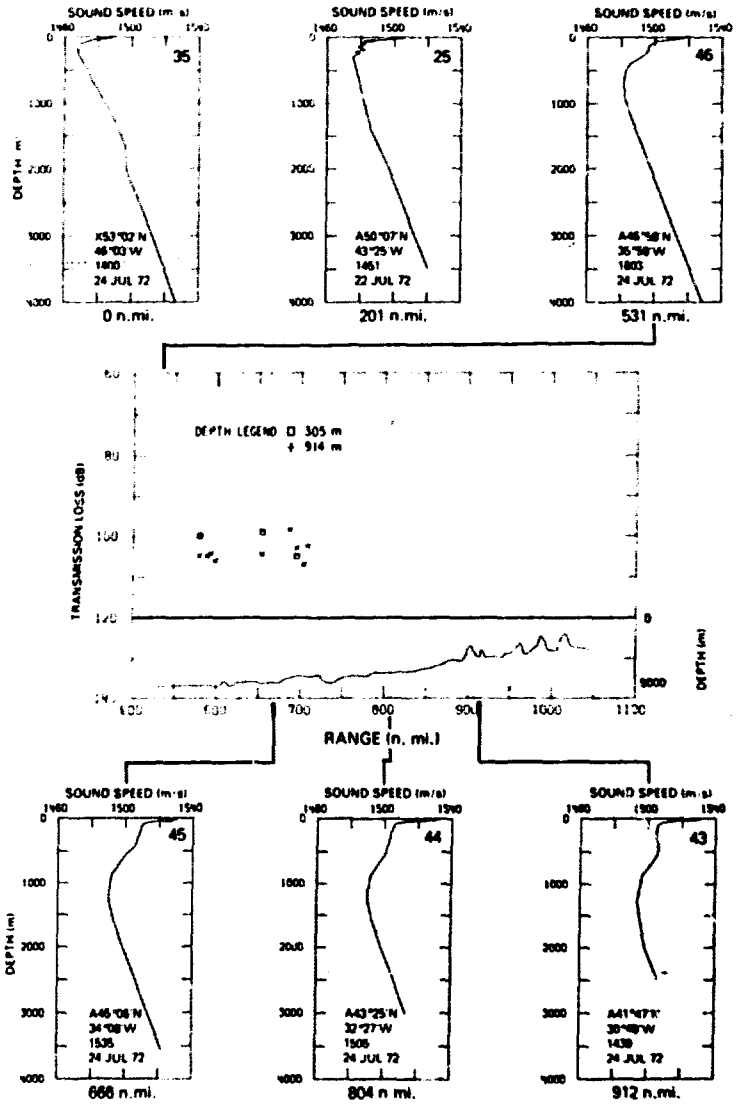

(C) Fig. A18 — Transmission loss from track 5A to the *Hayes* and sound-speed profiles

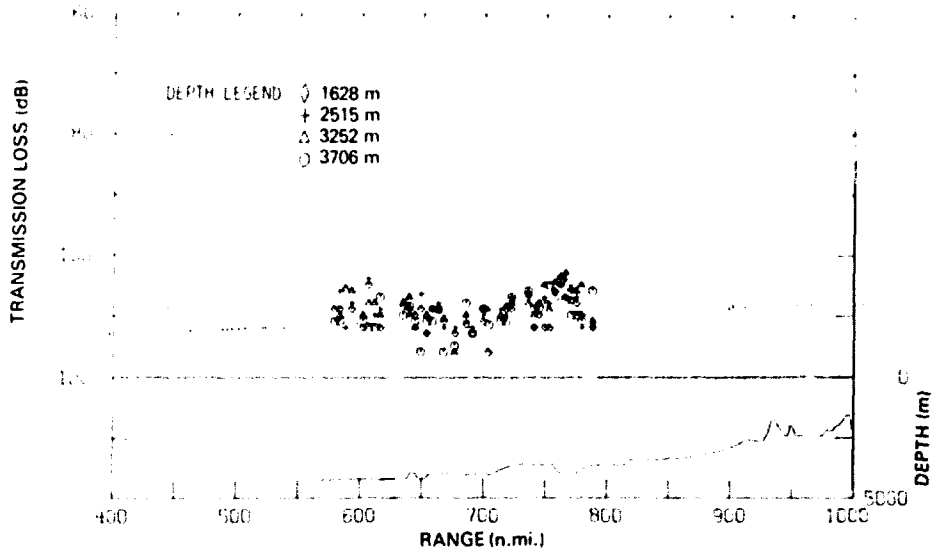

(U) Fig. A19 — Transmission loss from track 5A to the buoy

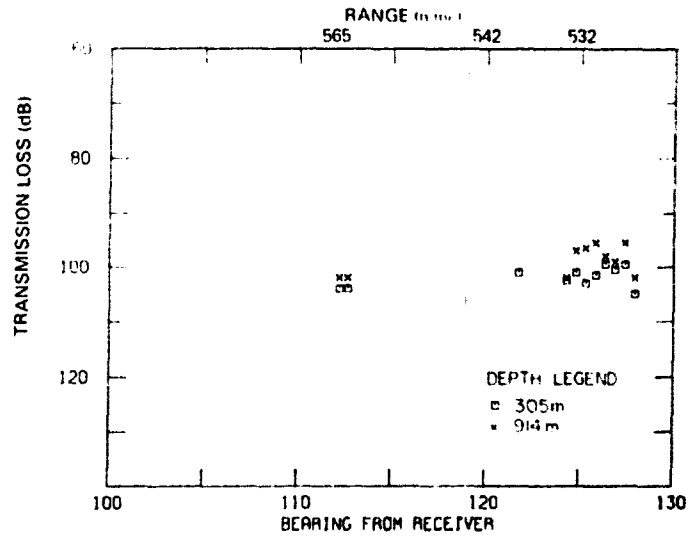

(U) Fig. A20 — Transmission loss from track 5B to the *Hayes*

(U) The transmission loss to the buoy is shown in Fig. A21. Data were obtained on the buoy because the high-level noise source near the *Hayes* did not affect the buoy and the bathymetric effect is discernable.

(C) The transmission losses for tracks 1C, 3B, 5A, and 5B lead to the conclusion that transmission loss to the south is poor for a shallow source; therefore the high ambient-noise levels observed are probably more heavily influenced by the shipping local to the Labrador Sea than would be expected. Hence fishing boats and other traffic along the Labrador coast, especially in the slope regions, may account for the high noise level. If so, the noise level and directional characteristics of the noise (which are expected to be seasonably dependent) can be incorporated in the design of a surveillance system to improve detection in the directions other than the source of noise. An additional

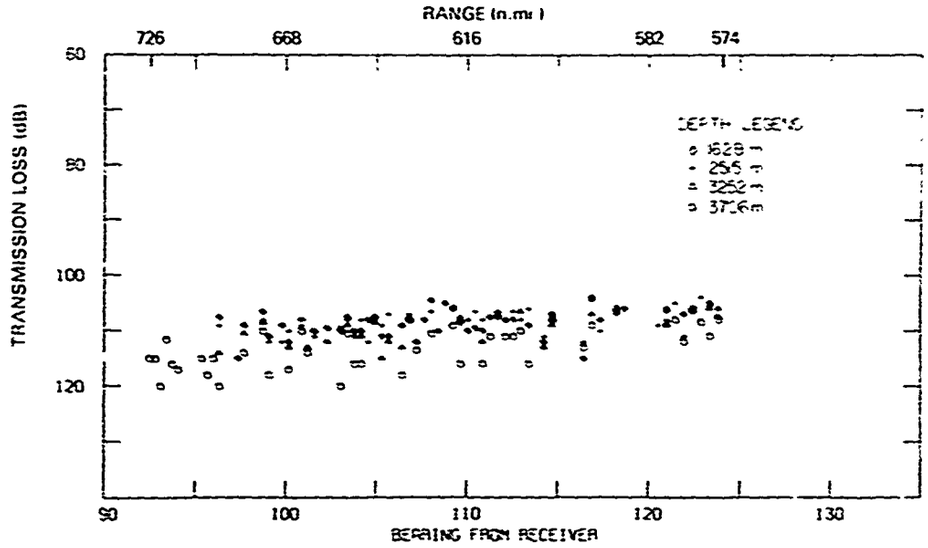

(U) Fig. A21 — Transmission loss from track 5B to the buoy

consideration is that a significant reduction in noise level would make targets in high-loss areas more visible, although the signals would continue to be sporadic.

TRACK 2

(U) Track 2 is a zigzag track toward the east which crosses the Mid-Atlantic ridge. Transmission loss as a function of range and the sound-speed profiles are shown in Fig. A22. At about 400 n.mi. the track crossed the Subarctic convergence and entered the highly variable bathymetry of the Charlie-*Gibbs* fracture zone and the foothills of the Mid-Atlantic ridge, leading to the greater variability in transmission loss beyond this range.

(C) The gap in the data on the 305-m-deep hydrophone between 200 and 400 n.mi. is due to an increase of self-noise level (by 7 dB) at the *Hayes*. A tape casualty is responsible for the gap for both hydrophones between 425 and 460 n.mi. Beyond 600 n.mi. data on both hydrophones were obscured by seismic interference. Shots dropped beyond the Mid-Atlantic ridge were blocked for the most part. What data were obtained showed losses greater than 100 dB. The transmission loss to the buoy is shown in Fig. A23. The gap from 460 to 540 n.mi. contains unacceptable SNR.

TRACK 6B

(C) When the data for track 6B were taken, the *Hayes* had taken a new position (30 n.mi. north of point D) and deployed only the 914-m-deep hydrophone due to intervening bad weather. Data were obtained out to a range of 413 n.mi., at which point excessive ship rolling and increased noise again precluded data processing. Shortly afterward, the aircraft terminated its operation due to weather conditions. This track runs

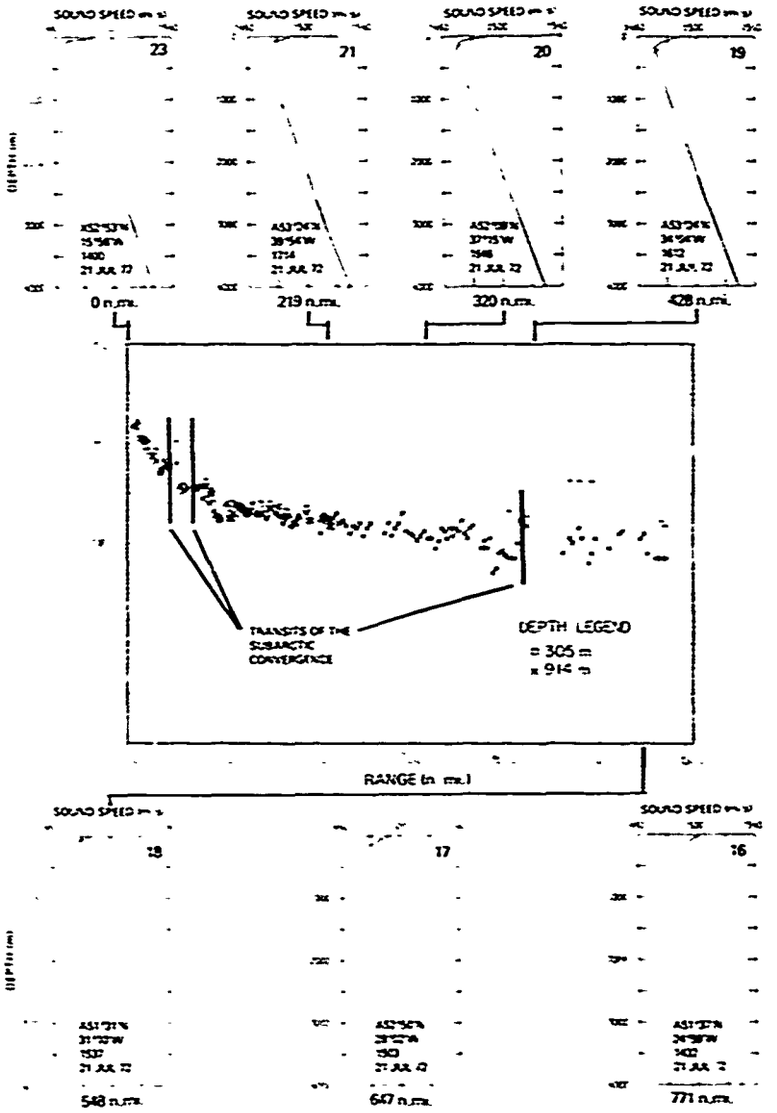

(C) Fig. A22 — Transmission loss from track 2 to the *Hayes* and sound-speed profiles

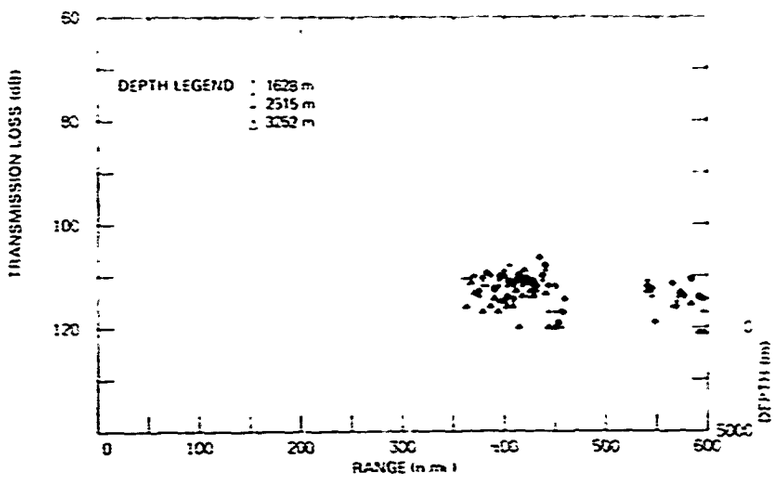

(U) Fig. A23 — Transmission loss from track 2 to the buoy

toward the Denmark strait (Figs. 1, 3, and 4) largely through the cold side of the Subarctic convergence except at point D. The sound-speed profiles and the transmission loss are plotted in Fig. A24. This transmission loss, when compared to that of track 1B (Fig A1) is less at the start, but rolls off more steeply with range, favoring to some extent transmission in the region extending up the the Davis strait. Thus moving a receiver further to the northeast than the experimental site should not affect the transmission loss in the direction of the Davis strait, while extending the detection range in the direction of the Denmark strait. The northerly movement may have a small (probably less than 2 dB) effect on transmission loss in southerly directions, dependent on the extent of the move. The buoy data were sparse on this track; however data illustrative of transmission loss to the buoy in this direction were obtained during track 8A.

TRACK 8A

(U) The transmission loss to only the buoy was obtained on track 8A (the *Hayes* had raised her hydrophones and was in transit for buoy pickup) and is given in Fig. A25. The apparent limiting at the lower end (120 dB) of the transmission-loss curve is the lower-limit setting of the shot processor. The bathymetry is essentially that for track 8B shown in Fig. A24.

TRACK 8B

(U) Although no track 8B data were analyzed for the buoy hydrophones, transmission from shots north of the 59°N parallel was consistently received at the two shallower depths.

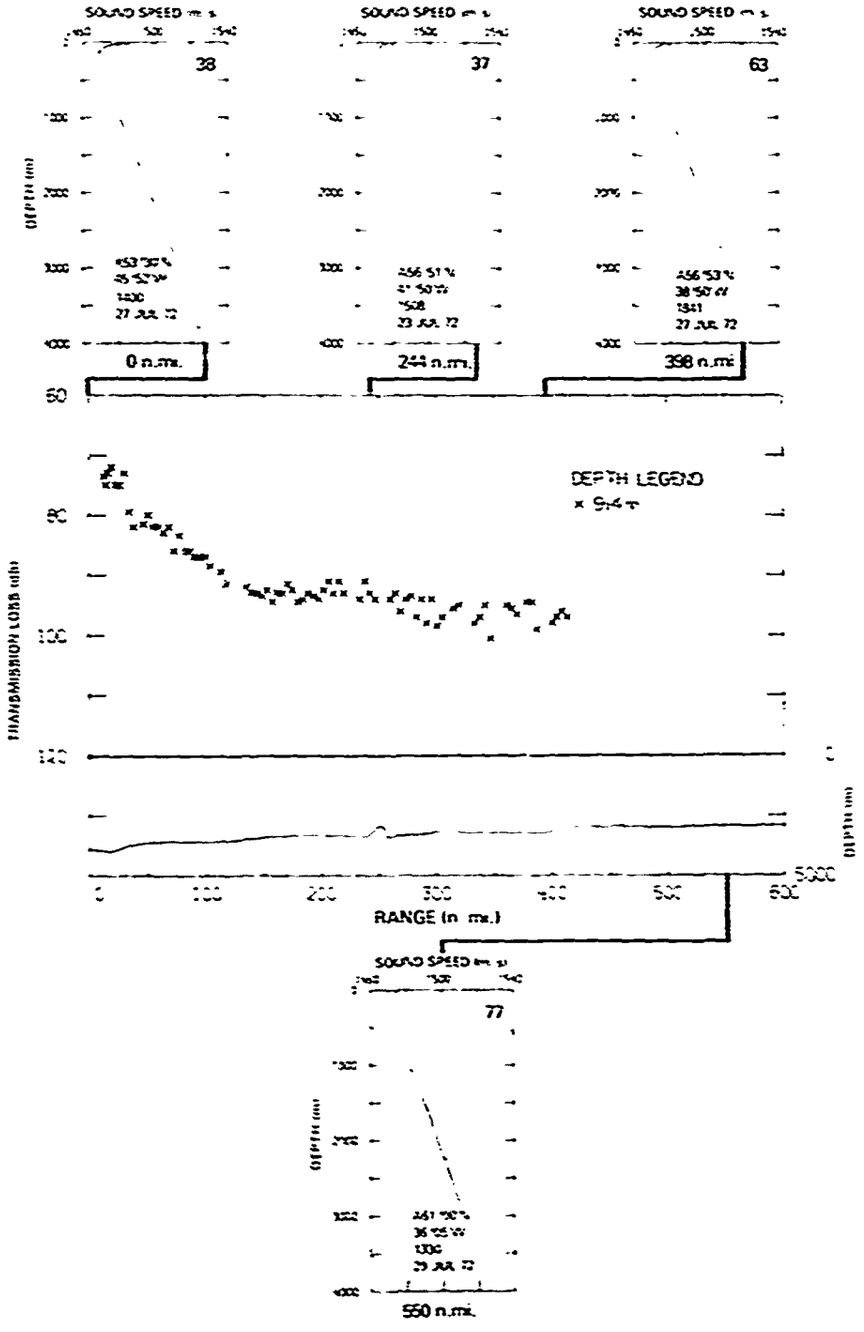

(C) Fig. A24 — Transmission loss from track 6B to the *Hayes* and sound-speed profiles

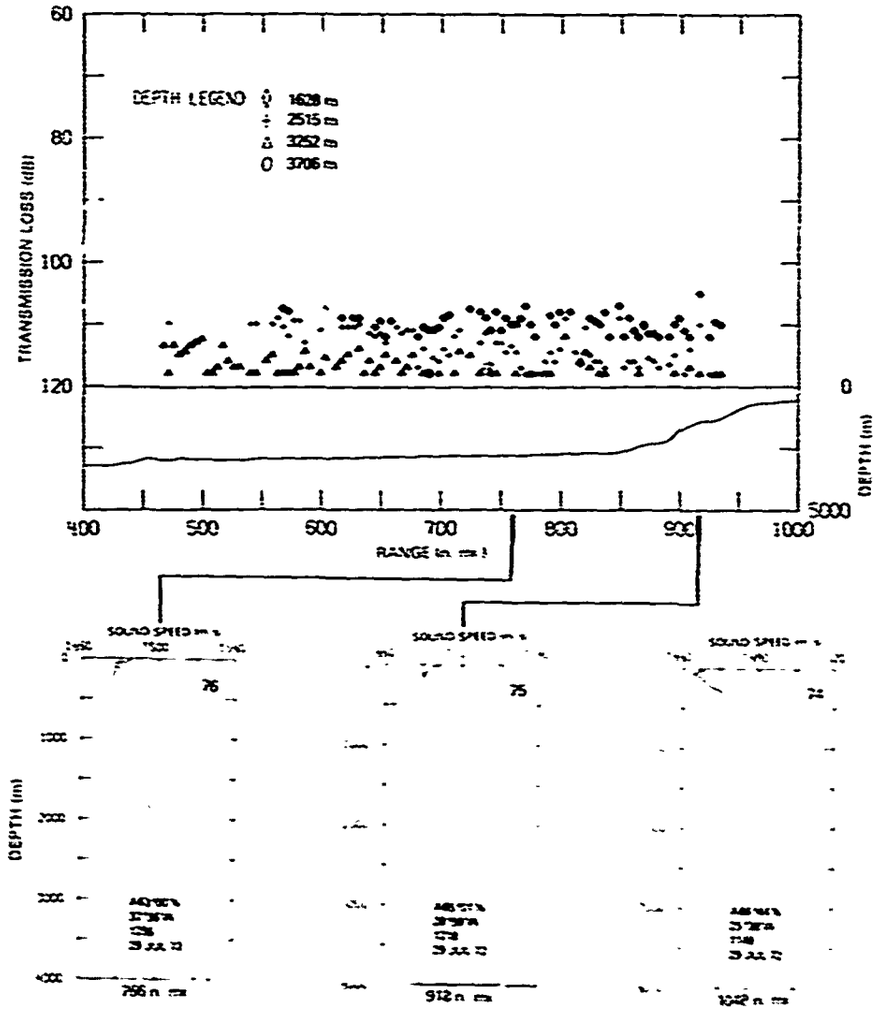

(C) Fig. A25 – Transmission loss from track SA to the buoy and sound-speed profiles

TRACKS 9A THROUGH 9C

(C) Tracks 9A through 9C were run in the absence of the *Hayes*, and although some transmission-loss data were obtained (111 to 119 dB) on the buoy hydrophones at depths of 1628 and 2515 m, seismic interference drastically limited the recoverable data. The data do indicate however that transmission beyond the Reykjanes ridge is generally blocked and shots are not seen east of the ridge, where the topography rises to 1829 m. This result implies that ambient noise sources east of the Labrador Sea are blocked by the ridge and is supported by ambient-noise measurements at locations south and north of the ridge's southern tip as reported in Ref. 2 of the main text.

REFERENCES

A1. C. F. Bassett and P. M. Wolff "Propagation Report No. 2" FNWC Technical Note 5S, Aug. 1970.

A2. FNWC Bottom Loss Area Chart for Atlantic Ocean, 15 Apr. 1969.

A3. W. B. Moseley, "Long Range, Low Frequency Acoustic Transmission Loss to Shetland" (U) Admiralty Research Laboratory, Teddington, Middlesex, ARL/0/R9, Jan. 1974 (Secret-Discrete).

(Page 38 Blank)

Appendix B [Confidential]
BATHYTHERMOGRAPH (AXBT AND XBT) DATA

(U) This appendix contains all of the data from expendable bathythermographs cast by the P3-C aircraft (AXBT's) and from expendable bathythermographs cast by the *Hayes* (XBT's). Table B1 lists the 85 AXBT's in an assigned numerical and chronological order giving latitude, longitude, data and time associated with each cast. Figure B1 shows, by its number, the location along the shot tracks where each AXBT was taken. The AXBT's are plotted in this numerical order in Figs. B2.

(U) Table B1 — AXBT Profiles for NORLANT 1972

No.	Latitude	Longitude	Date-Time-Group	No.	Latitude	Longitude	Date-Time-Group
1	64°29'N	56°21'W	201944 JUL 72	44	43°25'N	32°27'W	241505 JUL 72
2	62 55 N	59 48 W	202015 JUL 72	45	45 06 N	4 08 W	241535 JUL 72
3	61 00 N	56 45 W	202046 JUL 72	46	46 58 N	35 59 W	241603 JUL 72
4	59 04 N	54 26 W	202116 JUL 72	47	48 17 N	33 30 W	241631 JUL 72
5	57 20 N	51 55 W	202146 JUL 72	48	49 44 N	30 34 W	241701 JUL 72
6	55 36 N	49 31 W	202216 JUL 72	49	51 09 N	28 01 W	241727 JUL 72
7	53 54 N	47 17 W	202245 JUL 72	50	52 54 N	29 17 W	241753 JUL 72
8	52 00 N	45 52 W	202317 JUL 72	51	50 00 N	52 00 W	251206 JUL 72
9	49 50 N	46 00 W	202346 JUL 72	52	61 59 N	51 03 W	260043 JUL 72
10	47 04 N	46 00 W	210025 JUL 72	53	60 55 N	53 54 W	260108 JUL 72
11	48 17 N	48 45 W	210056 JUL 72	54	59 56 N	57 03 W	260136 JUL 72
12	48 45 N	49 36 W	210106 JUL 72	55	59 00 N	59 59 W	260201 JUL 72
13	57 00 N	22 03 W	211307 JUL 72	56	57 34 N	58 25 W	260221 JUL 72
14	55 03 N	22 07 W	211334 JUL 72	57	55 47 N	56 23 W	260245 JUL 72
15	53 06 N	22 11 W	211403 JUL 72	58	50 15 N	51 34 W	271532 JUL 72
16	51 37 N	24 59 W	211432 JUL 72	59	51 34 N	49 07 W	271600 JUL 72
17	52 50 N	28 02 W	211503 JUL 72	60	53 01 N	45 59 W	271634 JUL 72
18	51 31 N	31 10 W	211537 JUL 72	61	54 56 N	43 44 W	271738 JUL 72
19	53 24 N	34 04 W	211612 JUL 72	62	56 57 N	41 29 W	271810 JUL 72
20	52 09 N	37 15 W	211646 JUL 72	63	58 53 N	38 50 W	271841 JUL 72
21	53 24 N	39 54 W	211714 JUL 72	64	53 55 N	30 00 W	281424 JUL 72
22	53 08 N	51 00 W	221322 JUL 72	65	55 41 N	31 49 W	281502 JUL 72
23	53 02 N	47 29 W	221351 JUL 72	66	57 20 N	33 25 W	281528 JUL 72
24	51 58 N	44 58 W	221421 JUL 72	67	58 59 N	35 22 W	281553 JUL 72
25	50 07 N	43 25 W	221451 JUL 72	68	60 22 N	31 40 W	281622 JUL 72
26	48 16 N	41 53 W	221521 JUL 72	69	61 39 N	28 22 W	281652 JUL 72
27	46 15 N	40 13 W	221553 JUL 72	70	62 58 N	25 04 W	281718 JUL 72
28	44 17 N	38 35 W	221623 JUL 72	71	63 42 N	28 19 W	281742 JUL 72
29	42 26 N	37 02 W	221652 JUL 72	72	64 18 N	31 35 W	281805 JUL 72
30	40 28 N	35 23 W	221723 JUL 72	73	64 58 N	34 48 W	281827 JUL 72
31	39 59 N	33 18 W	221747 JUL 72	74	66 44 N	25 38 W	291148 JUL 72
32	46 09 N	30 05 W	221819 JUL 72	75	65 01 N	28 59 W	291218 JUL 72
33	52 1 N	53 09 W	231301 JUL 72	76	63 00 N	32 36 W	291255 JUL 72
34	54 57 N	51 31 W	231331 JUL 72	77	61 00 N	36 05 W	291330 JUL 72
35	57 02 N	49 34 W	231405 JUL 72	78	58 59 N	39 18 W	291404 JUL 72
36	57 04 N	46 07 W	231432 JUL 72	79	58 44 N	39 39 W	291413 JUL 72
37	56 51 N	41 50 W	231508 JUL 72	80	56 19 N	31 57 W	291516 JUL 72
38	54 04 N	41 22 W	231622 JUL 72	81	58 01 N	30 30 W	291545 JUL 72
39	49 03 N	42 34 W	231746 JUL 72	82	59 40 N	29 01 W	291606 JUL 72
40	49 09 N	45 57 W	231816 JUL 72	83	60 59 N	30 03 W	291625 JUL 72
41	49 05 N	50 07 W	231858 JUL 72	84	62 00 N	31 00 W	291641 JUL 72
42	40 02 N	29 03 W	241411 JUL 72	85	62 45 N	29 41 W	291653 JUL 72
43	41 47 N	30 49 W	241439 JUL 72				

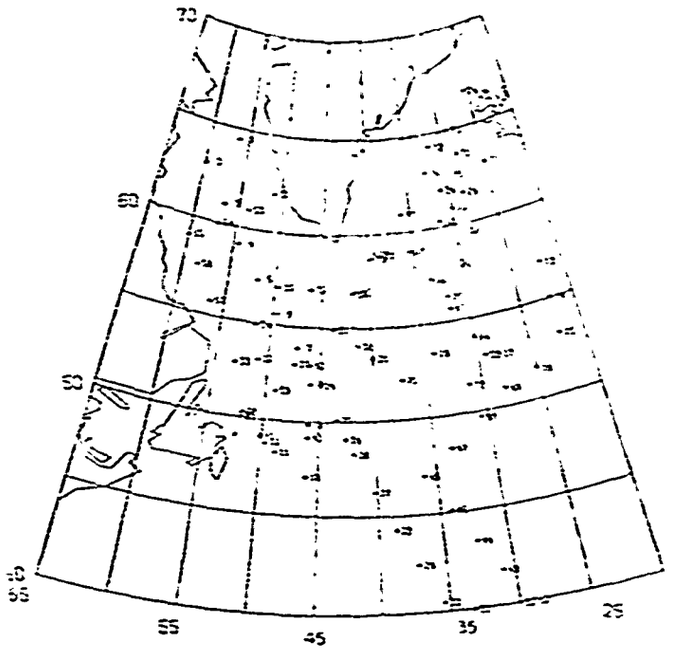

(C) Fig. B1 — Location of AXBT profiles

(U) Table B2 lists the XBT data taken from the *Hayes* with position, day, and time data. They are plotted in numerical order in Figs. B3.

(U) The temperature-salinity curves used to convert the temperature data of Figs. B2 and B3 to the sound-speed profiles of Appendix A were retrieved [B1] from archival temperature-salinity data and applied to each temperature profile of a given location and data. Each sound-speed profile of Appendix A is identified with an X and the number to correspond to the XBT profile from which it is derived or is identified with an A and the number to correspond to the AXBT profile from which it is derived. The extension of the sound-speed profiles beyond the termination of the temperature data is obtained by fitting appropriate deep-Nansen-cast archival data to the measured data.

REFERENCE

B1. B. G. Roberts, Jr., "Retrieval Program for Archival Nansen-Cast Data," NRL Report 7633, Oct. 1973 (Unclassified).

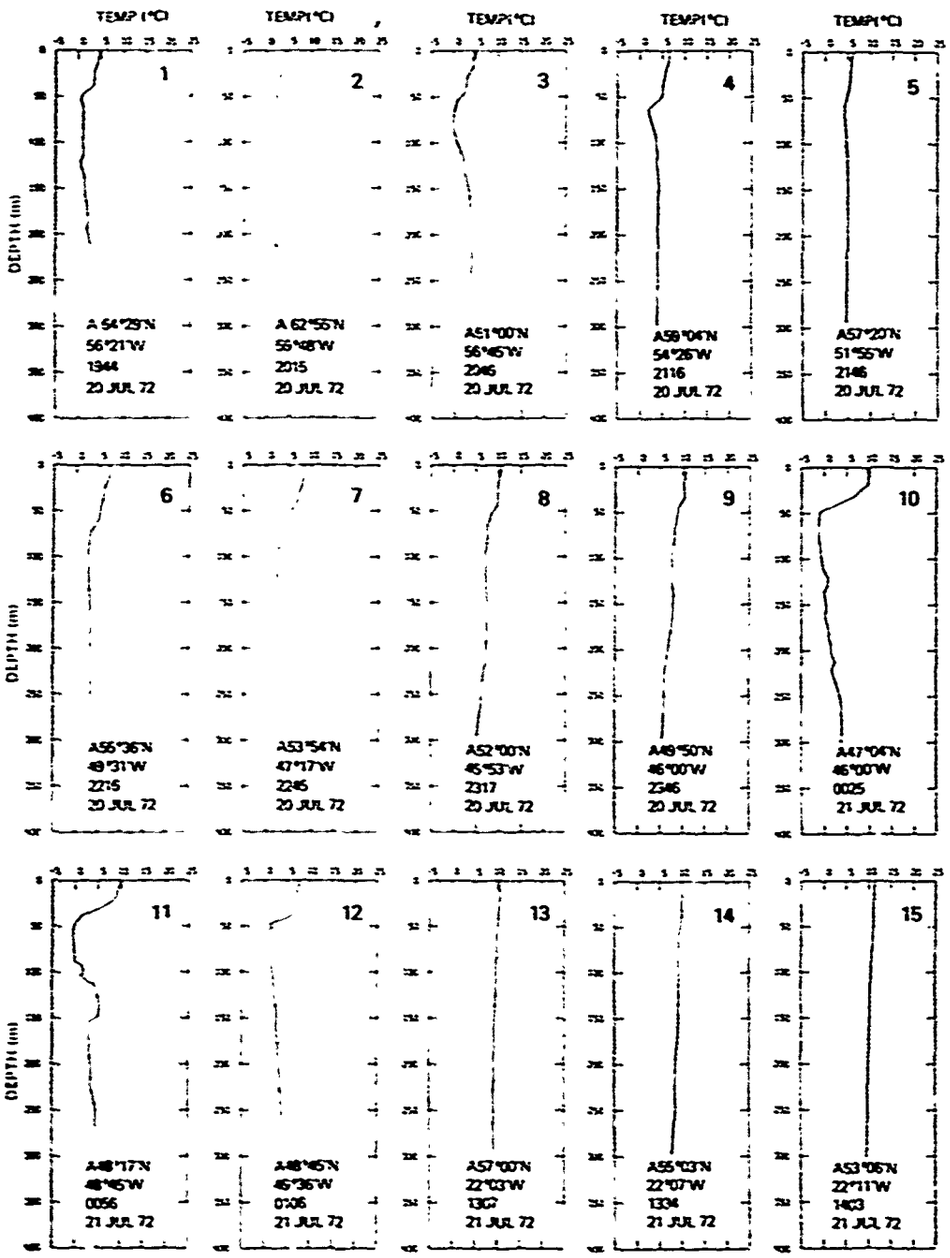

(U) Fig. B2a — AXBT profiles 1 through 15

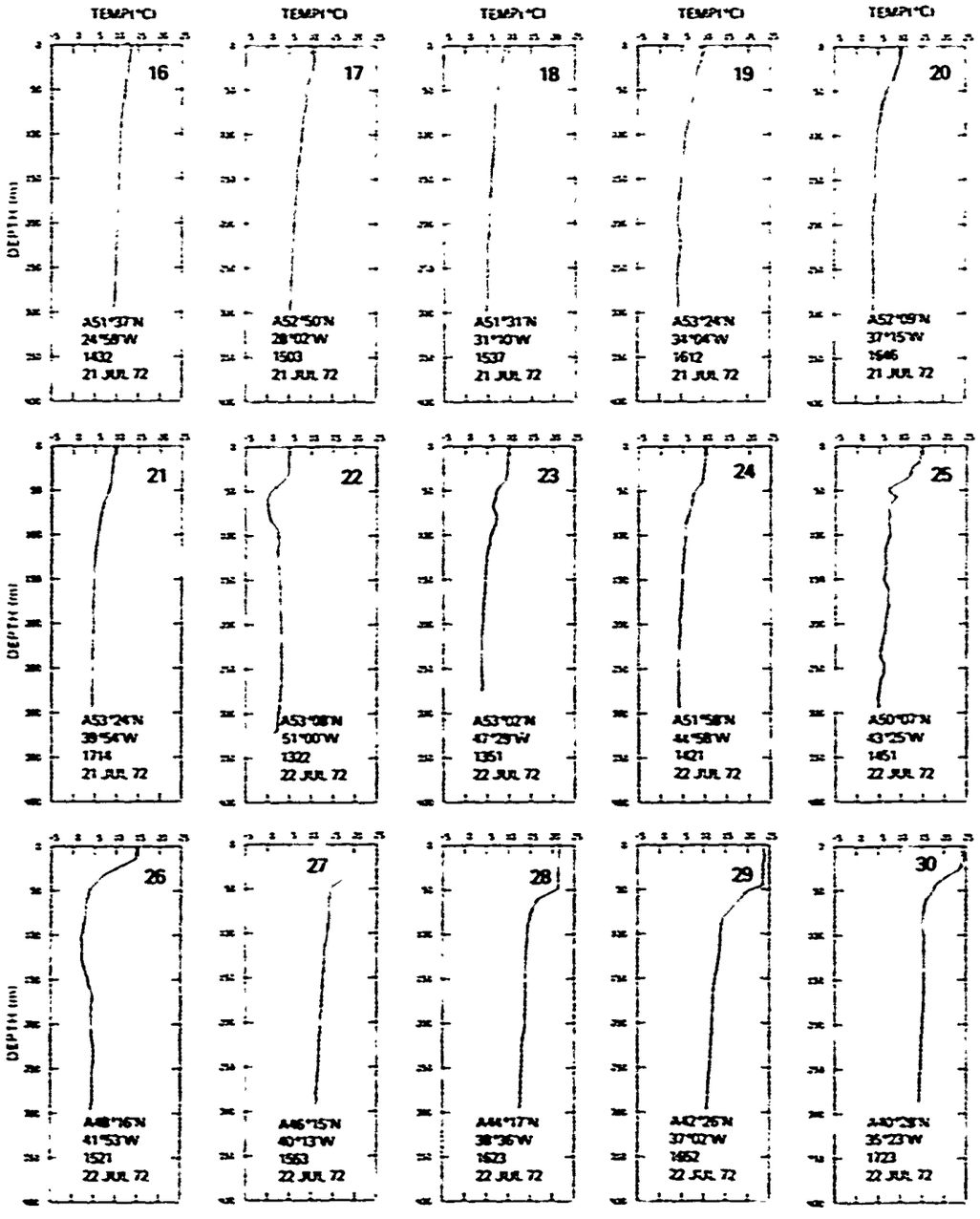

(U) Fig. B2b — AXBT profiles 16 through 30

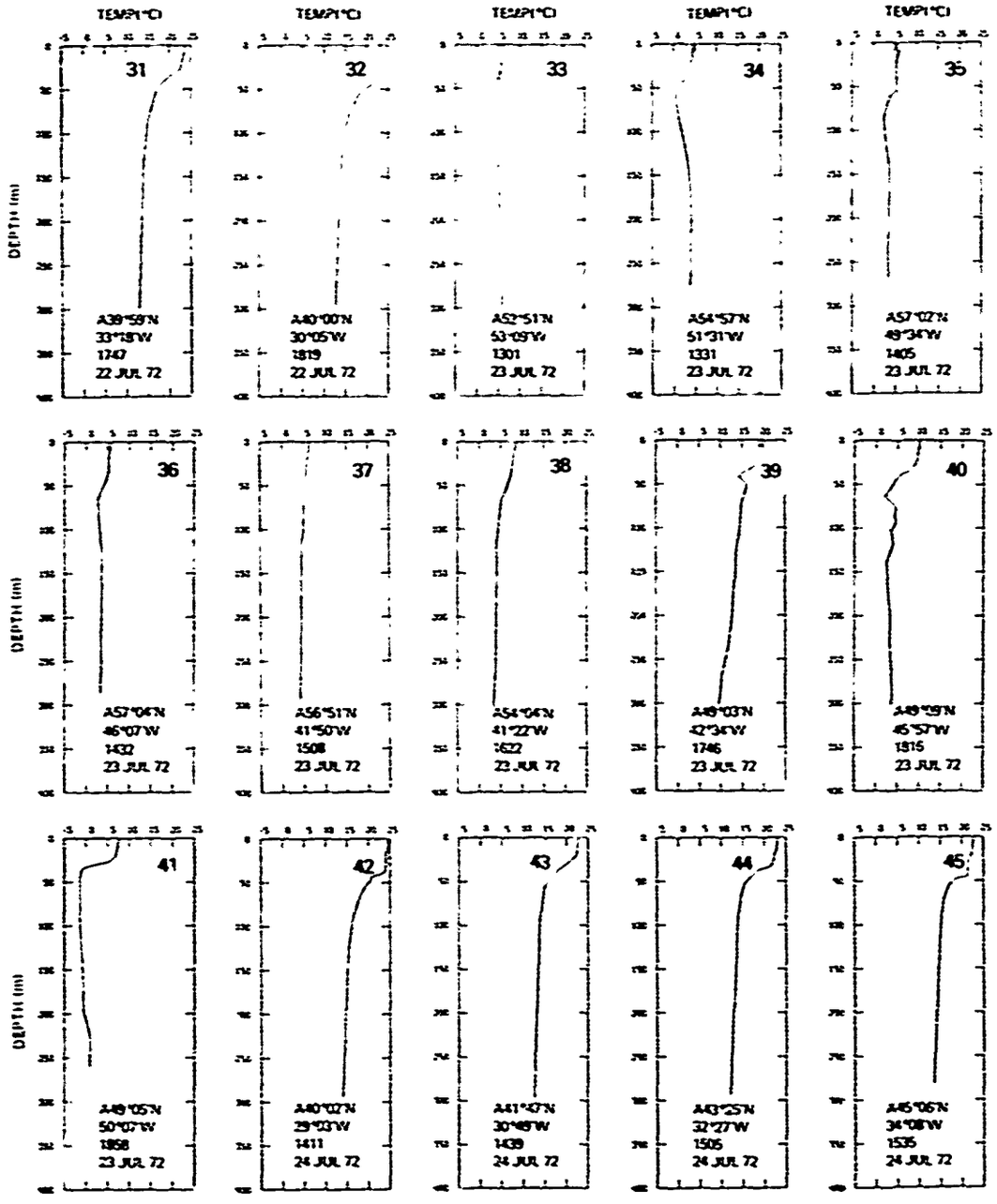

(U) Fig. B2c — AXBT profiles 31 through 45

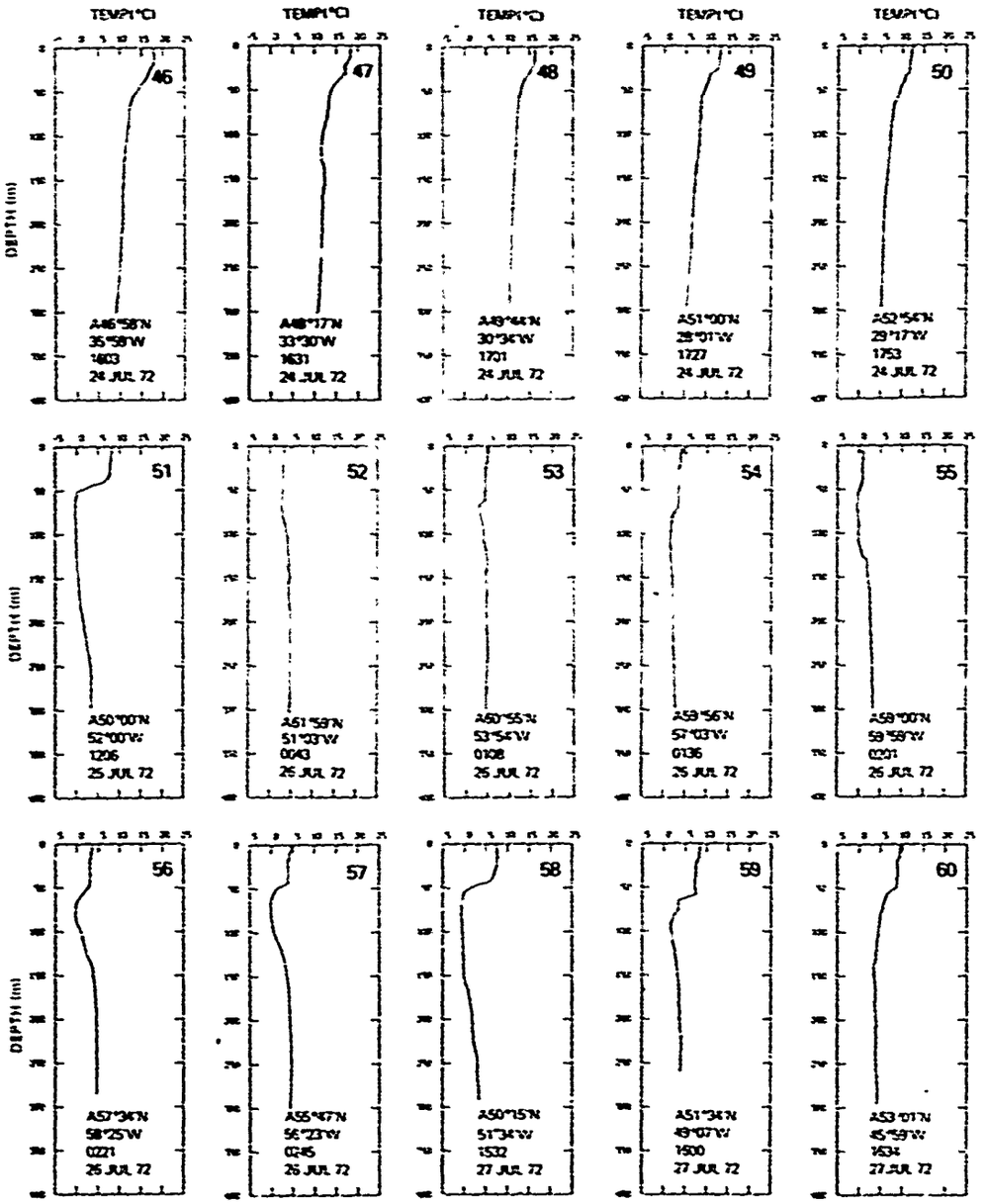

(U) Fig. B2d – AXBT profiles 46 through 60

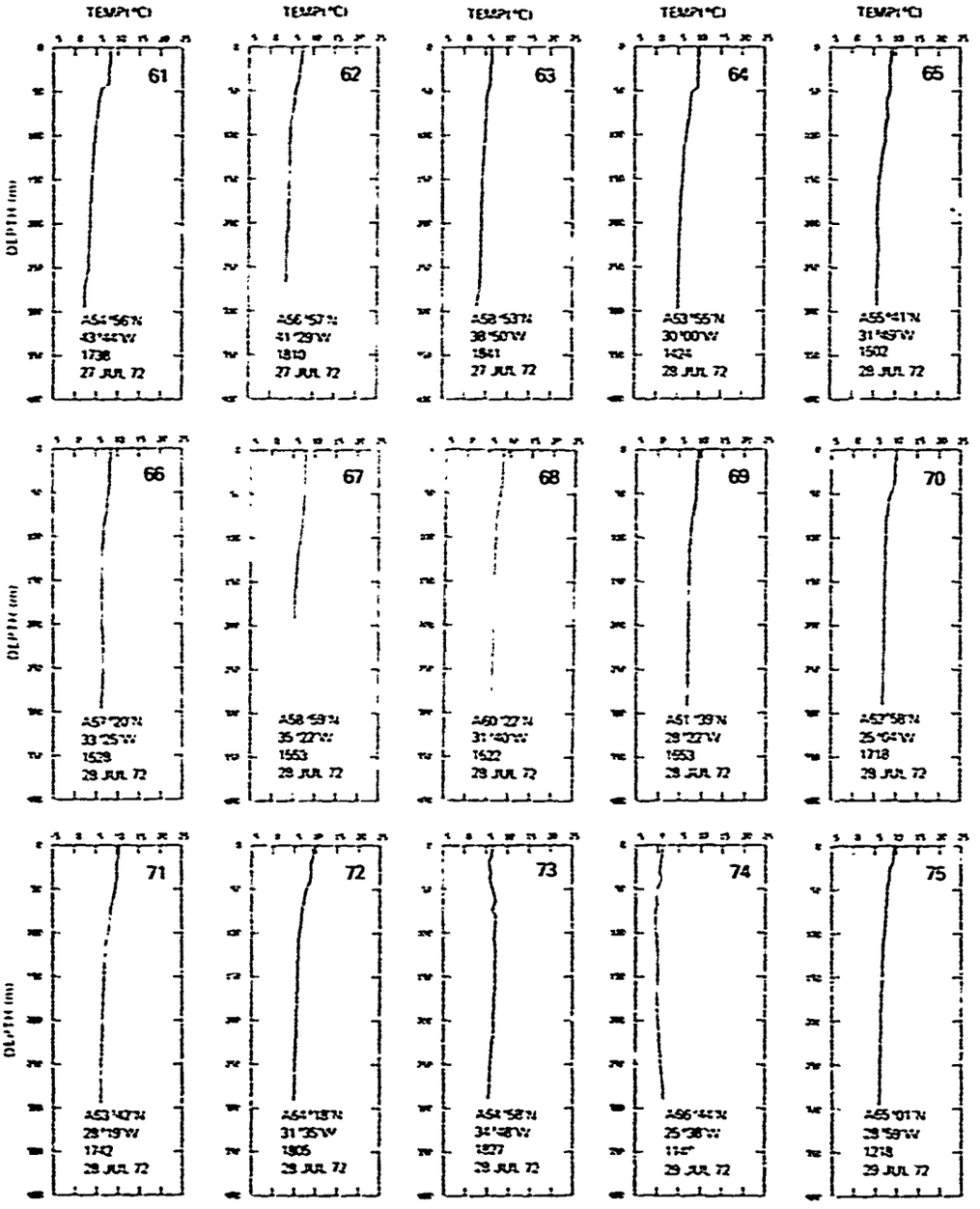

(U) Fig. B2e — AXBT profiles 61 through 75

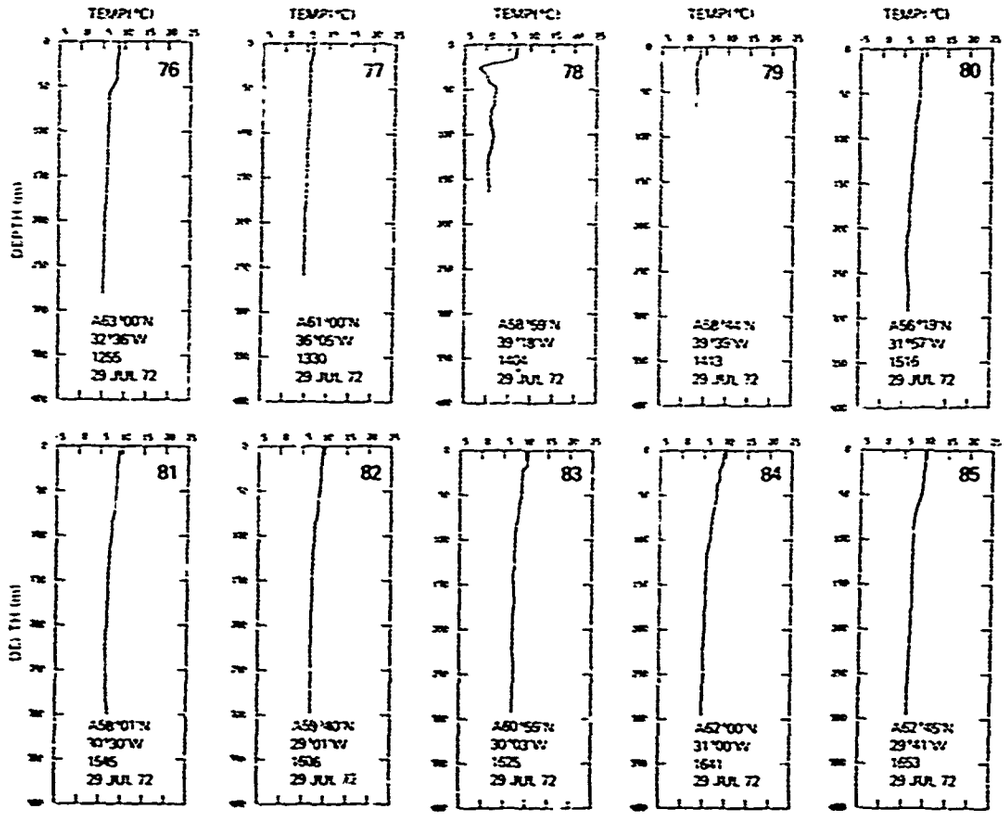

(U) Fig. B2f — AXBT profiles 76 through 85

(U) Table B2 — *Hayes* XBT Profiles for NORLANT 1972

No.	Latitude	Longitude	Date-Time-Group
1	50°13′N	47°50′W	152000 JUL 72
2	51 06 N	43 25 W	160400 JUL 72
3	51 32 N	45 54 W	160803 JUL 72
4	52 02 N	45 08 W	161215 JUL 72
5	52 28 N	45 04 W	170000 JUL 72
6	53 13 N	45 04 W	170400 JUL 72
7	53 53 N	44 59 W	170800 JUL 72
8	54 04 N	45 12 W	172009 JUL 72
9	54 03 N	45 13 W	172025 JUL 72
10	53 42 N	46 04 W	180000 JUL 72
11	53 18 N	46 57 W	180420 JUL 72
12	52 57 N	47 49 W	181200 JUL 72
13	52 55 N	47 37 W	182000 JUL 72
14	52 57 N	46 57 W	190000 JUL 72
15	52 58 N	46 17 W	190400 JUL 72
16	52 57 N	46 00 W	190800 JUL 72
17	53 04 N	45 59 W	191500 JUL 72
18	52 59 N	45 55 W	200219 JUL 72
19	52 57 N	45 53 W	200800 JUL 72
20	52 56 N	45 55 W	201800 JUL 72
21	52 54 N	45 55 W	210000 JUL 72
22	52 55 N	45 57 W	210800 JUL 72
23	52 53 N	45 56 W	211400 JUL 72
24	52 55 N	45 58 W	212140 JUL 72
25	53 00 N	45 57 W	220200 JUL 72
26	53 04 N	46 14 W	220800 JUL 72
27	53 00 N	45 58 W	221410 JUL 72
28	53 02 N	46 01 W	222045 JUL 72
29	53 03 N	46 02 W	230200 JUL 72
30	53 01 N	45 58 W	230800 JUL 72
31	53 01 N	45 59 W	231415 JUL 72
32	53 01 N	46 00 W	232000 JUL 72
33	53 01 N	46 02 W	240200 JUL 72
34	53 03 N	46 03 W	240800 JUL 72
35	53 02 N	46 03 W	241400 JUL 72
36	53 01 N	46 02 W	242000 JUL 72
37	53 01 N	46 01 W	250200 JUL 72
38	53 30 N	45 52 W	271400 JUL 72
39	53 30 N	45 54 W	272000 JUL 72
40	54 02 N	45 07 W	280200 JUL 72
41	54 02 N	45 05 W	280830 JUL 72
42	54 09 N	45 07 W	281430 JUL 72
43	53 57 N	45 05 W	282000 JUL 72
44	53 57 N	45 04 W	290200 JUL 72
45	53 57 N	45 04 W	290800 JUL 72
46	52 59 N	47 42 W	292000 JUL 72
47	53 02 N	47 47 W	301400 JUL 72
48	53 48 N	47 47 W	310200 JUL 72
49	53 57 N	44 53 W	022000 AUG 72
50	54 06 N	41 41 W	030400 AUG 72
51	54 08 N	40 25 W	030800 AUG 72
52	54 13 N	30 33 W	031200 AUG 72
53	54 16 N	36 54 W	031600 AUG 72
54	54 29 N	32 06 W	040400 AUG 72
55	54 36 N	30 25 W	040800 AUG 72

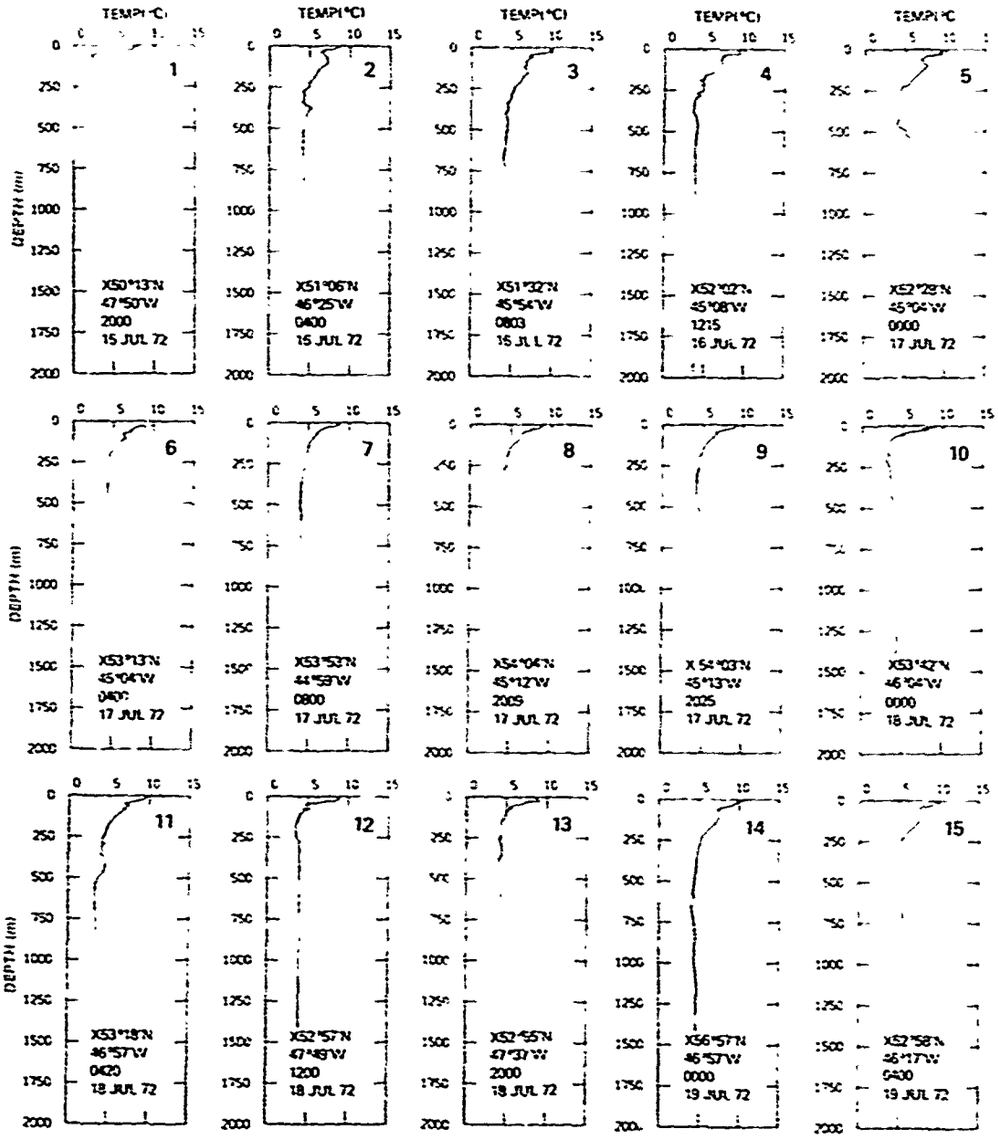

(U) Fig. B3a — XBT profiles 1 through 15

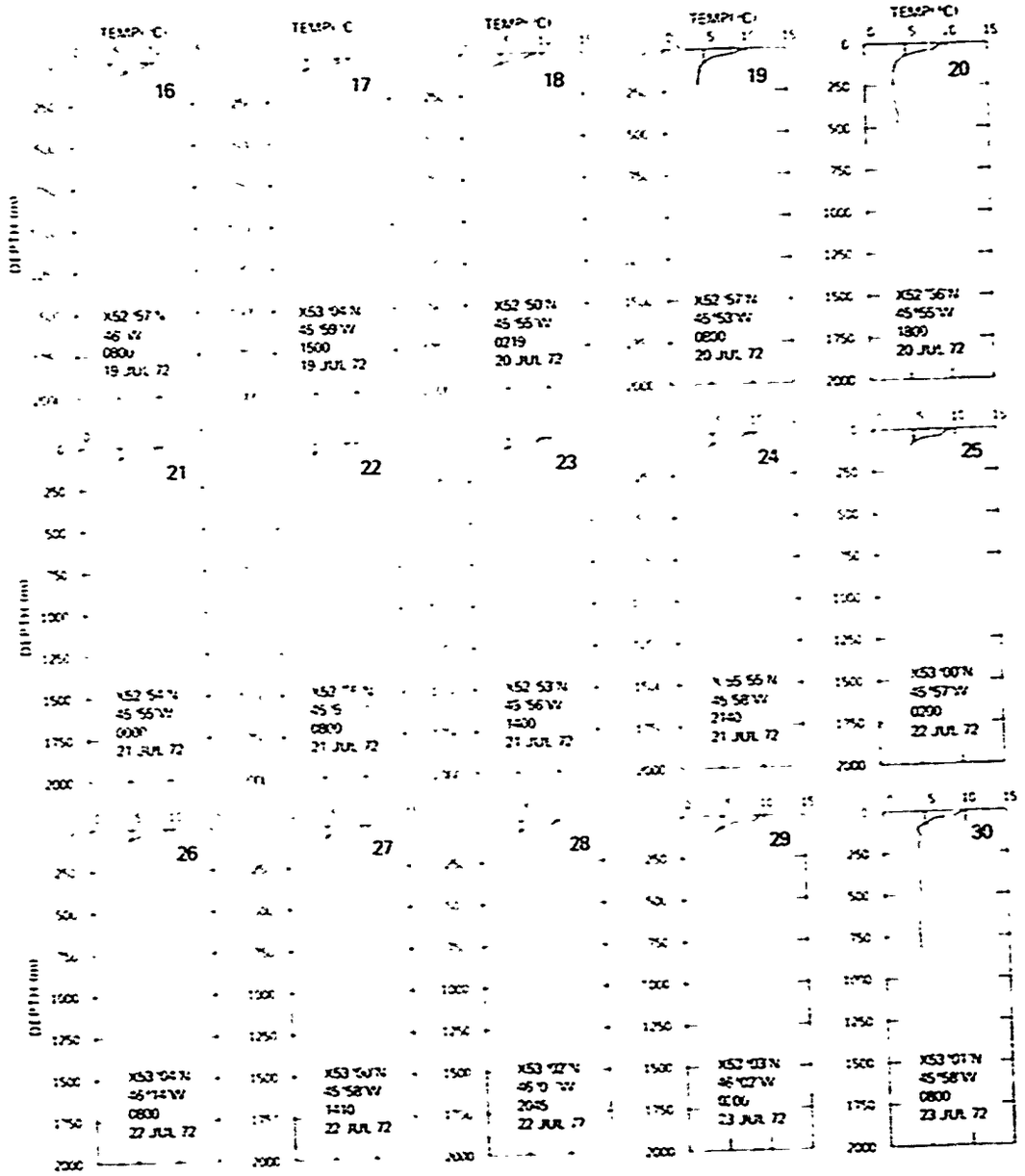

(U) Fig. B3b — XBT profiles 16 through 30

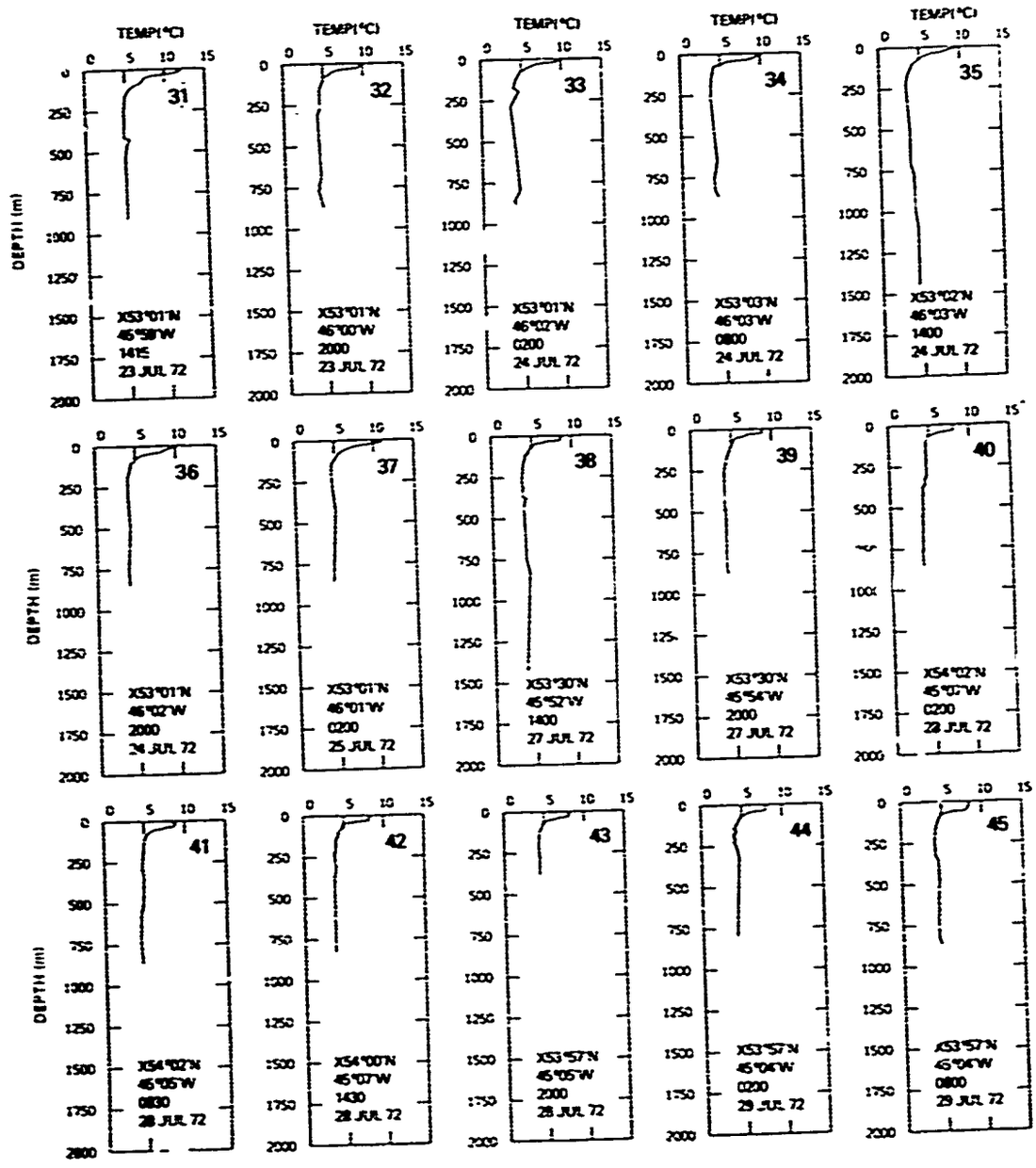

(U) Fig. B3c – XBT profiles 31 through 45

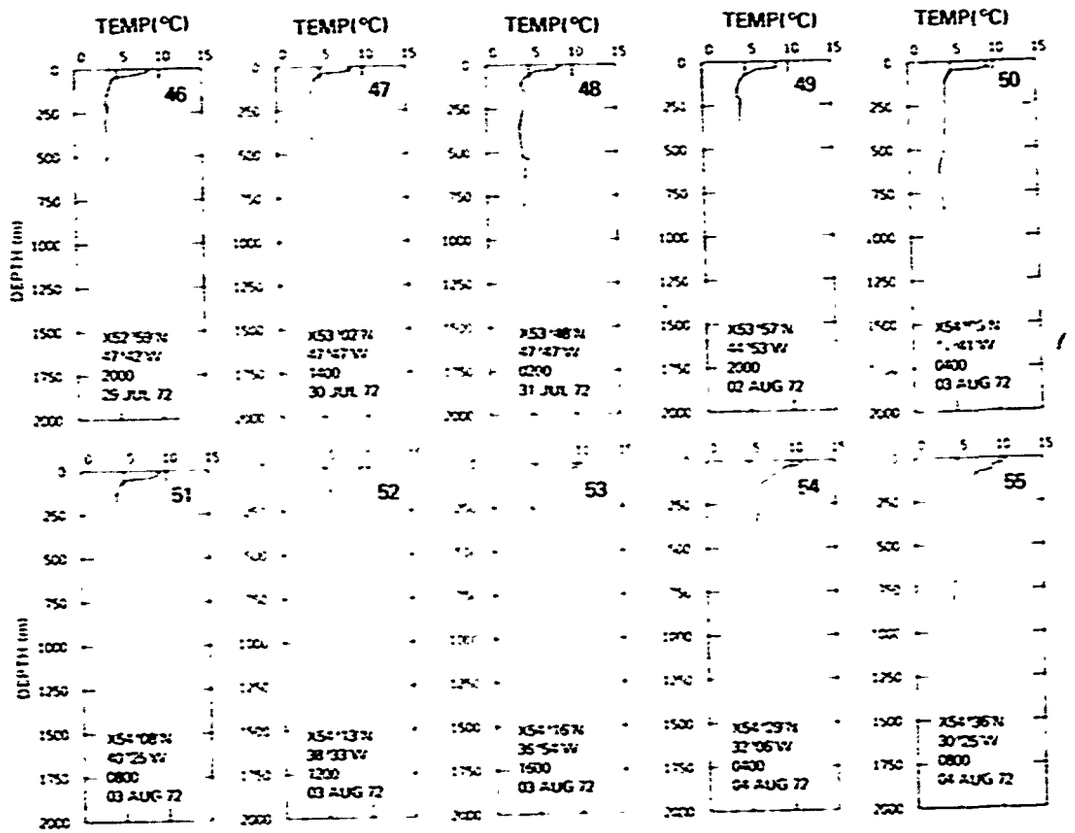

(U) Fig. B3d — XBT profiles 46 through 55

Appendix C [Unclassified]
KEFLAVIK OPERATIONS AND THE TACTICAL SUPPORT CENTER

In the conduct of NORLANT 1972, phase I, two dedicated P3-C aircraft and three crews of Patrol Squadron Twenty-four (VP-24) under COMFAIRWING ELEVEN OF COMFAIRWINGSLANT were used to deploy "Signals, Underwater Sound" (SUS) charges, and AN/SSQ-36 sonobuoys (AXBT's) and to provide information on surface-ship contacts along the tracks flown. Fourteen flights were made, with an NRL participant aboard, including ten data flights during 19-29 July, using air bases at Sondre Stromfjord (Sondrestrom), Greenland; Goose Bay, Labrador; Lajes, Azores; and Keflavik, Iceland, as staging areas. Only 85.5 hours of flight time was required, including a pre-position flight to Sondrestrom, two supportive flights, and one test flight after a casualty, providing 10720 n.mi. out of the 12860 n.mi. of data track listed in the Exercise Plan.

In addition there was a separate P3-C flight, a mail drop, to Jan Mayen island, with the NRL-Keflavik team aboard for orientation and to obtain a measure of SUS reliability. (This examination of SUS lots for performance was based upon a sobering encounter with defective SUS's during NEAT II when a similar exercise was conducted out of Rota in 1971.) The plans for this examination of performance were to deploy Mk 54 Mark 61 SUS's set to detonate at a depth of 18.3 m, with 18 to be deployed altitude of 152 m on a 3-n.mi.-diameter circle about an AN/SSQ 41 sonobuoy with a hydrophone at 18.3 m and 18 to be deployed from an altitude of 305 m on a 5-n.mi.-diameter circle about the sonobuoy. A planned 610-m drop of 18 SUS's was not conducted due to weather, and instead the 152-m altitude was repeated. The Mark 61 SUS's were all of one lot, all consisting of the same body, fins, and explosive. Six Mark 82 SUS's of two different lots were deployed to detonate at 91.4 m in a double drop with the Mark 61 SUS's, similar to the double drops of the scheduled exercise. The results were that there was one dud out of the six Mark 82 SUS's and one dud and two only-booster firings out of the 54 Mark 61 SUS's. These ratios reaffirmed the decision to emphasize the shallower shots during the scheduled exercise.

Because of discrepancies in the exact position of the sonobuoy, the elapsed travel time for ranges between the sonobuoy and the shot impact point could not be determined in order to compute individual sink rates. However the time differences between the 18.3-m and 91.4-m SUS detonations are independent of this correction, and they averaged 13 seconds, yielding a sink rate of 5.6 m/s. These differences are lower than the nominal 17 ± 3 seconds which are obtained from the sink times of 3 ± 1 and 20 ± 2 seconds that are listed [C1] for the shallow and deep depths. The smaller differences indicate that the deeper shots were going off at shallower depths than set for. However, listed [C1] sink rates of 6.9 and 5.1 m/s for the shallow and deep shots encompass the value obtained. During the exercise 2440 Mark 61 SUS's with a detonation depth of 18.3 m, were dropped, one a minute, and 150 Mark 82 SUS's, with a detonation depth of 91.4 m, were dropped, one each 15 minutes. The P3-C flights were conducted under visual flight rules generally at altitudes of 305 m to insure that SUS charges were not deposited onto any ice floes, icebergs, or ships.

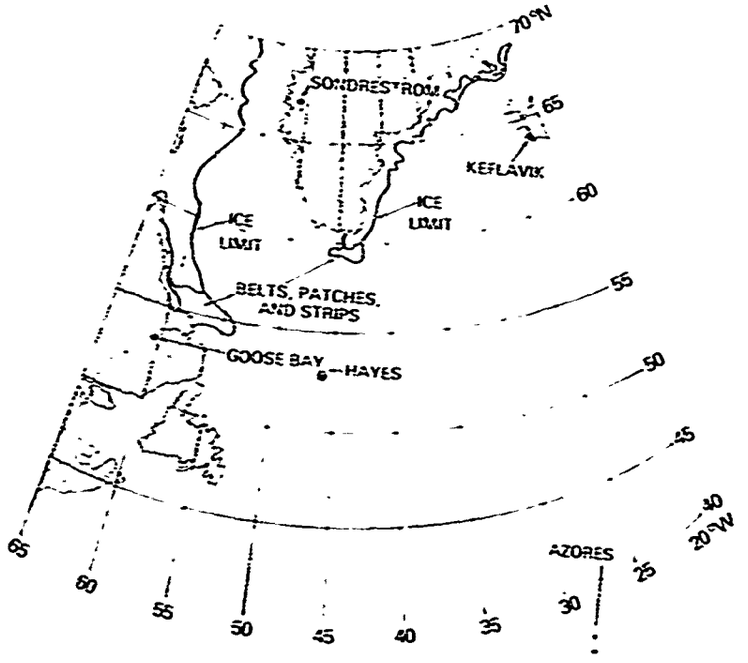

Fig. C1 — Southern ice limit on 17 July 1972 (based on a chart from the Fleet Weather Facility, Suitland)

The altitude from which the SUS charges were deployed changed (from 122 m to as much as 914 m) during the exercise to reflect conditions of visibility. Nonetheless the SUS charges were deployed one each minute, with ground speed generally about 260 knots. Time late in a drop was noted, and all changes in course, speed, and altitude were reflected in a computed shot impact point such that horizontal range and bearing to each receiving sensor was obtained with each shot.

The extent of ice belts remaining along the east coast of Greenland and off Labrador is shown in Fig. C1. Each P3-C was modified [C2] in the field for the temporary installation of eight identical crew boxes at various deck locations carrying from 33 to 66 SUS charges each, depending on weight distribution requirements, holding a total of 384 SUS charges, for a load of 1240 kilograms.

During execution of the SUS tracks, 91 AXBT's were deployed, with 85 of these being acceptable, sampling the ocean environment down to 305 m at track turning points and/or every 1/2 hour. These data were analog-recorded on a 25.4-mm magnetic tape by the AQH-4 recorder aboard and displayed on-line as a trace (Fig. C2a) from a Rustrak recorder and as a gram (Fig. C2b) on an AQA-7 unit. Each P3-C carries two inertial navigation systems (ASN-84), providing a complete and automatic log of navigation data (the course true heading, speed, and altitude into the digital in-flight recorder, part of the AYA-8 peripheral system) every 4 seconds as controlled by the onboard ASQ-114 computor. Included in this record are on-demand entries for a SUS/sonobuoy drop, radar contacts, and the digitized AXBT thermal data. During the flight a high-speed printer

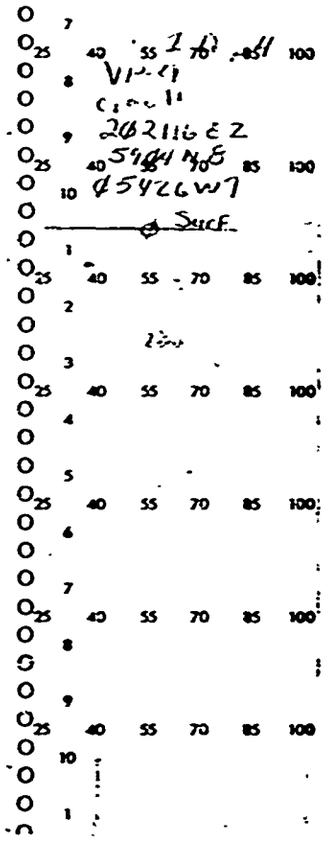

Fig. C2a — Typical on-line AXBT plot on a Rustrak recorder

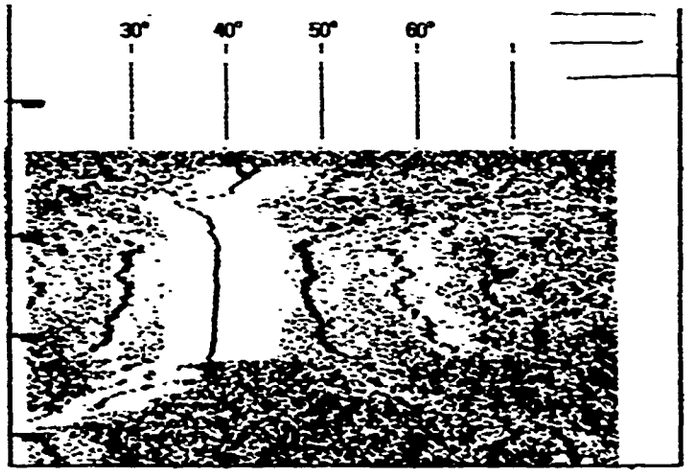

Fig. C2b — Typical on-line AXBT plot as a gram on a AQA-7

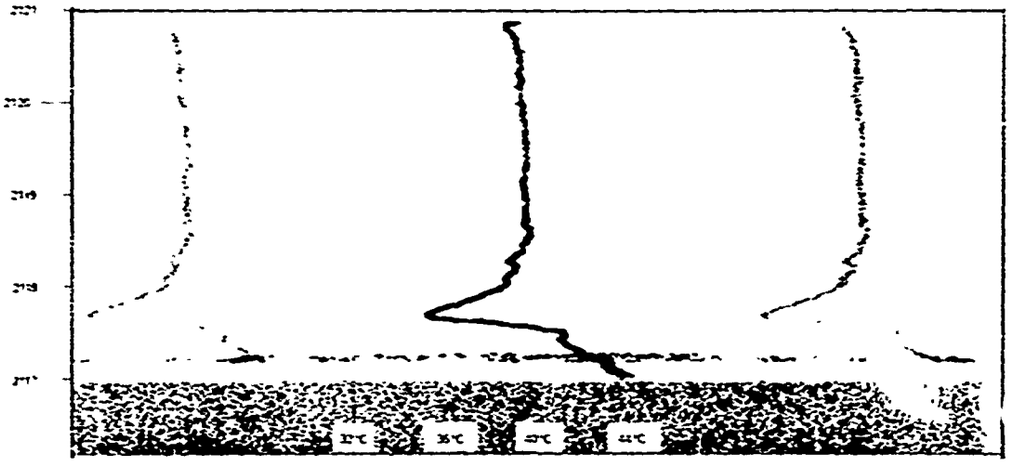

Fig. C3 — Typical off-line-processed AXBT plot as a gram

could provide the navigation parameters (usually provided at the 15-minute mark, corresponding to the drop of a Mark 81 SUS, and at the deployment of an AXBT).

After a P3-C returned to Keflavik, the analog tape from the AQH-4 and the digital tape produced by the navigation systems and events computor were processed at the Tactical Support Center (TSC). With use of this digital tape, a complete mission replay of the tracks flown and events logged was obtained with the facilities at TSC. One of the four remote CRT display consoles was used to obtain access to any time/function segment of the mission and to obtain optional outputs in the form of CRT track displays and readouts, 0.76-m drum plots of the radar contacts or buoy deployments, high-speed page printouts containing navigation data every 1, 5, or 10 minutes, as desired, or lists all the radar contacts or buoy events and the digitized temperatures corresponding to the Rustrak record.

An examination of the Rustrak analog record revealed that the temperature structure is often difficult to resolve. In addition, the on line gram record, although an improvement in resolving temperature, was not much better in depth extent than the Rustrak. The off-line digitized temperature records were also not of acceptable quality. Thus it was decided to generate an improved thermal-structure display by using the Advanced Fast Time Acoustic Analysis System at TSC with an 8:1 speedup ratio as outputted on one of the lofargram units. A detailed record is produced (Fig. C3) and was analyzed to obtain the thermal structures illustrated in Appendix B.

Other data abstractions included the AXBT locations and the positions and plots of the radar contacts along the aircraft track. The radar contacts were provided to Raif Associates for inclusion in the shipping-surveillance section (section V-a) of the preliminary report [C3].

REFERENCES

C1. Technical Manual NAVAIR 11-1-107, Nov. 1973.

C2. Patrol Squadron Twenty Four letter 20:sec, 300 Serial 448 of 19 Oct. 1972 (Unclassified).

C3. B. B. Adams and R. L. Martin, editors, NORLANT '72 Preliminary Report (Confidential), Vol. II — Appendices (Unclassified), 9 Feb. 1973.

*U.S. GOVERNMENT PRINTING

DEPARTMENT OF THE NAVY
OFFICE OF NAVAL RESEARCH
875 NORTH RANDOLPH STREET
SUITE 1425
ARLINGTON VA 22203-1995

IN REPLY REFER TO:

5510/1
Ser 321OA/011/06
31 Jan 06

MEMORANDUM FOR DISTRIBUTION LIST

Subj: DECLASSIFICATION OF LONG RANGE ACOUSTIC PROPAGATION PROJECT (LRAPP) DOCUMENTS

Ref: (a) SECNAVINST 5510.36

Encl: (1) List of DECLASSIFIED LRAPP Documents

1. In accordance with reference (a), a declassification review has been conducted on a number of classified LRAPP documents.

2. The LRAPP documents listed in enclosure (1) have been downgraded to UNCLASSIFIED and have been approved for public release. These documents should be remarked as follows:

   Classification changed to UNCLASSIFIED by authority of the Chief of Naval Operations (N772) letter N772A/6U875630, 20 January 2006.

   DISTRIBUTION STATEMENT A: Approved for Public Release; Distribution is unlimited.

3. Questions may be directed to the undersigned on (703) 696-4619, DSN 426-4619.

BRIAN LINK
By direction

Subj: DECLASSIFICATION OF LONG RANGE ACOUSTIC PROPAGATION PROJECT (LRAPP) DOCUMENTS

DISTRIBUTION LIST:

NAVOCEANO (Code N121LC – Jaime Ratliff)
NRL Washington (Code 5596.3 – Mary Templeman)
PEO LMW Det San Diego (PMS 181)
DTIC-OCQ (Larry Downing)
ARL, U of Texas
Blue Sea Corporation (Dr.Roy Gaul)
ONR 32B (CAPT Paul Stewart)
ONR 321OA (Dr. Ellen Livingston)
APL, U of Washington
APL, Johns Hopkins University
ARL, Penn State University
MPL of Scripps Institution of Oceanography
WHOI
NAVSEA
NAVAIR
NUWC
SAIC

Declassified LRAPP Documents

Report Number	Personal Author	Title	Publication Source (Originator)	Pub. Date	Current Availability	Class.
TIRC1871976F	Hoffmann, J., et al.	CHURCH ANCHOR AMBIENT NOISE FINAL REPORT (U)	Texas Instruments, Inc.	750901	ADC070512; NS; AU; ND	C
Unavailable	Unavailable	SQUARE DEAL ANALYSIS EXECUTIVE SUMMARY (U)	University of Texas, Applied Research Laboratories	751001	AU	C
Unavailable	Unavailable	SQUARE DEAL ENVIRONMENTAL ACOUSTIC SUMMARY SEC. IV-SIGNAL PROPAGATION (U)	Xonics, Inc.	751101	AU	C
Unavailable	Unavailable	CHURCH ANCHOR CW PROPAGATION LOSS AND SIGNAL EXCESS REPORT (U) PRELIMINARY	Texas Instruments, Inc.	751201	AU	C
SAN-BBOP-76-U127. B38485	Unavailable	MSS CONFIGURED ACODAC SYSTEMS FINAL ENGINEERING REPORT (U)	Sanders Associates, Inc.	760115	ND	C
Unavailable	Unavailable	MSS CONFIGURED ACODAC SYSTEMS PRELIMINARY TEST REPORT-BEARING STAKE (U)	Sanders Associates, Inc.	761111	AU	C
ARL-TR-76-52	Watkins, S. L.	MOORED SURVEILLANCE SYSTEM FIELD VALIDATION TEST AMBIENT SOUNDFIELD AND PROPAGATION MEASUREMENTS FOR NEAR-BOTTOM SENSORS AT SITE A3 (U)	University of Texas, Applied Research Laboratories	761201	ND	C
Unavailable	Unavailable	REAL-WORLD MEASUREMENTS Of MSS ACODAC HYDROPHONE RESPONSE PATTERNS (U) PHASE REPORT - PRELIM DRAFT	Naval Air Development Center	761222	AU ADC 010980	C
XONICSTR109OSD	Morey, C. F.	EFFECT OF ARRAY TILT ON BEAM NOISE, SIGNAL-TO-NOISE RATIO, AND DETECTION OPPORTUNITY	Xonics, Inc.	770101	NS; ND	C
NRL-7996	Andriani, C. R., et al.	ACOUSTIC PROPAGATION IN THE LABRADOR SEA	Naval Research Laboratory	770308	ADC010061 ND	C
Unavailable	Gabrielson, T. B.	REAL-WORLD MEASUREMENTS Of MSS ACODAC HYDROPHONE RESPONSE PATTERNS	Naval Air Development Center	770601	ADC010980	C
NAVSO P970V27, NO. 3	Del Balzo, D. R.	TOWED ARRAY DYNAMICS AND ACOUSTIC IMPLICATIONS (U)	Office of Naval Research	770701	ND	C
WHOI-77-55	Baxter, L.	MSS-FVT ACODAC DATA ASSESSMENT AND AMBIENT NOISE THIRD OCTAVE DATA PROCESSING (U)	Woods Hole Oceanographic Institution	770801	AU; ND	C
Unavailable	Unavailable	LARGE APERTURE MARINE BASIC DATA ARRAY (LAMBDA) SYSTEM DESCRIPTION	Naval Ocean R&D Activity	770901	AU	C
Unavailable	Unavailable	CHURCH STROKE REVIEW (U)	University of Texas, Applied Research Laboratories	770912	AU	C
NOSCTR169	Yee, G. S.	BEARING STAKE EXERCISE PRELIMINARY RESULTS (U) RESEARCH AND DEVELOPMENT REPORT OF JAN-MAY 77	Naval Ocean Systems Center	771031	NS; AU; ND	C
LRAPPRC77020	Palumbo, J. X., et al.	LRAPP EXERCISE ACOUSTIC DATA INVENTORY DECEMBER 1977 (U)	Naval Ocean R&D Activity	771201	NS; ND	C

ENCL (1)